Atmospheric Research 164–165 (2015) 142–155

Contents lists available at ScienceDirect

Atmospheric Research

journal homepage: www.elsevier.com/locate/atmos

Identification of aerosol types over an urban site based on air-mass trajectory classification

G.V. Pawar [a], P.C.S. Devara [b], G.R. Aher [a,*]

[a] Atmospheric Physics Research Laboratory, Physics Department, Nowrosjee Wadia College, Pune 411 001, India
[b] Amity Centre for Ocean-Atmospheric Science and Technology (ACOAST), Amity University Haryana Manesar, Gurgaon 122413, India

ARTICLE INFO

Article history:
Received 20 December 2014
Received in revised form 28 March 2015
Accepted 29 April 2015
Available online 12 May 2015

Keywords:
AOD
Ångström exponent
Long range transport
Air-mass
Aerosol types

ABSTRACT

Columnar aerosol properties retrieved from MICROTOPS II Sun Photometer measurements during 2010–2013 over Pune (18°32′N; 73°49′E, 559 m amsl), a tropical urban station in India, are analyzed to identify aerosol types in the atmospheric column. Identification/classification is carried out on the basis of dominant airflow patterns, and the method of discrimination of aerosol types on the basis of relation between aerosol optical depth ($AOD_{500\ nm}$) and Ångström exponent (AE, α). Five potential advection pathways viz., NW/N, SW/S, N, SE/E and L have been identified over the observing site by employing the NOAA-HYSPLIT air mass back trajectory analysis. Based on AE against $AOD_{500\ nm}$ scatter plot and advection pathways followed five major aerosol types viz., continental average (CA), marine continental average (MCA), urban/industrial and biomass burning (UB), desert dust (DD) and indeterminate or mixed type (MT) have been identified. In winter, sector SE/E, a representative of air masses traversed over Bay of Bengal and Eastern continental Indian region has relatively small AOD ($\tau_{p\lambda} = 0.43 \pm 0.13$) and high AE ($\alpha = 1.19 \pm 0.15$). These values imply the presence of accumulation/submicron size anthropogenic aerosols. During pre-monsoon, aerosols from the NW/N sector have high AOD ($\tau_{p\lambda} = 0.61 \pm 0.21$), and low AE ($\alpha = 0.54 \pm 0.14$) indicating an increase in the loading of coarse-mode particles over Pune. Dominance of UB type in winter season for all the years (i.e. 2010–2013) may be attributed to both local/transported aerosols. During pre-monsoon seasons, MT is the dominant aerosol type followed by UB and DD, while the background aerosols are insignificant.

1. Introduction

Aerosols are a fundamental part of the Earth's atmosphere with numerous impacts on the Earth's radiation budget and hydrological cycle. These effects are not yet fully understood (Forster et al., 2007; Penner et al., 2011; Bond et al., 2013). The main reason for this is the large variability and limited knowledge of the temporal and spatial distribution of the optical and microphysical properties of aerosols on global scales (Penner et al., 2001; Kaskaoutis et al., 2010). On account of this, the accurate assessment of the aerosol impact on the radiative transfer is a complex task, since various aerosol types cause different effects on the spectral distribution of solar radiation (Kaskaoutis and Kambezidis, 2008). Hence, a detailed knowledge of the optical properties of the key aerosol types is highly essential. Globally, numerous studies have been carried out to identify different aerosol types and to characterize their properties at several observing sites (Ramanathan et al., 2001; Dubovik et al., 2002; Moorthy et al., 2005, 2009; Jayaraman et al., 2006; Pace et al., 2006; Kaskaoutis et al., 2007a,b; El-Metwally et al., 2008; Ogunjobi et al., 2008; Kalapureddy et al., 2009; Babu et al., 2011; Sinha et al., 2011, 2012; Chakravarty et al., 2011; Pathak et al., 2012; Kulkarni et al., 2012; Padmakumari et al., 2013; Kanike et al., 2014). Based on these measurements, aerosols can be grouped into four main types viz., forest and grassland fire produced biomass burning aerosols, urban/industrial aerosols from fossil fuel combustions in populated urban/industrial regions, windblown desert dust injected into the atmosphere and marine aerosols (Kaskaoutis et al., 2007a). A realistic characterization of aerosol properties can be carried out by employing strong spectral dependence of both AOD and AE (Holben et al., 2001). Therefore, these two parameters are widely used to identify different aerosol types over the globe (Kaskaoutis et al., 2007b).

The aerial transport of aerosols (either in solid or liquid phase) involves different spatial and temporal scales. Although, the origin of the aerosols may lie in different continents, a time span of the order of 3 days to 1 month may be sufficient for aerosols to disperse to any part of the globe (Stohl et al., 2002a,b). This is regarded as the long-range transport (LRT) and is a direct consequence of atmospheric currents, which necessitate the use of a certain amount of energy. For this to happen, the atmosphere is considered as a huge self-regulated heat machine that transports energy all over the globe and controls the climatic system (Fraile et al., 2006). Earlier, it was noticed that the AOD and other aerosol properties are largely influenced by the regional

* Corresponding author at. Atmospheric Physics Research Laboratory, Physics Department, Nowrosjee Wadia College, Pune 411 001, India.

http://dx.doi.org/10.1016/j.atmosres.2015.04.022
0169-8095/

and/or synoptic scale air-mass types (Moorthy et al., 1991; Smirnov et al., 1994, 2002; Pillai and Moorthy, 2001; Kabashnikov et al., 2014; Aher et al., 2014).

Backward trajectory analysis is a commonly used tool to identify synoptic scale atmospheric transport patterns and/or determine the origin of air pollutants (Dorling et al., 1992; Cape et al., 2000; Stohl et al., 2002a,b; Jorba et al., 2004; Cabello et al., 2008). The transport of atmospheric compounds and aerosols from a source to receptor sites can be easily understood with the help of back trajectories, as they trace the path of a polluted air parcel backward in time and space and have been used to track the history/ pathways of air parcels arriving at a specific location (Fleming et al., 2012). Back-trajectory analysis was employed to qualitatively link variations in the chemical and optical properties of aerosols to sources like broadly biomass burning and fossil fuel combustion located in geographical regions traversed by air masses arriving in the Arabian Sea and tropical Indian Ocean (Reiner et al., 2001; Mayol-Bracero et al., 2002; Quinn et al., 2002; Franke et al., 2003). Examples may include quantifying ground-level aerosol concentrations (Sa'nchez et al., 1990; Rodriguez et al., 2001), examining the relationship between air-mass history and trace elements (Bahrmann and Saxena, 1998; Cape et al., 2000; Methven et al., 2001) and investigating the relationship between air-mass type and AOD (Vergaz et al., 2002, 2005; Estelle's et al., 2007). Many other studies have used back-trajectories for the interpretation of how aerosols or other atmospheric components vary over space and time (e.g., Smirnov et al., 1995; Querol et al., 2002; Heintzenberg et al., 2003; Pérez et al., 2004; Toledano et al., 2006; Dı'az et al., 2006; Gorchakov et al., 2014; Kabashnikov et al., 2014).

Large-scale spatial and temporal heterogeneities of aerosol sources and the complex pathways of aerosol transport are a major impediment in the straightforward assessment of their regional and global impacts on the earth's climate (Kim and Ramanathan, 2008; Kaskaoutis et al., 2009). The understanding of LRT of aerosols and their vertical extent is important in studies related to the estimation of radiative forcing (Badarinath et al., 2008). Moreover, along with aerosol physico-optical properties, the atmospheric chemical composition is also strongly influenced by LRT (Lelieveld et al., 2002; Pace et al., 2006). Therefore, there is an increase in the awareness of the potential of air-mass trajectories in advecting aerosols from distinct source regions and causing changes in the optical depth or composition or physical characteristics at far off locations (Tyson et al., 1996; Krishnamurti et al., 1998; Moorthy et al., 2001, 2003; Kaskaoutis et al., 2014).

In the present work, we make the first-ever attempt to investigate and to identify the prime pathways favoring the presence of specific aerosol types over a tropical urban station, Pune. Different aerosol types are also discriminated by using $AOD_{500\ nm}$ and AE values retrieved in the spectral interval 440–870 nm. For this, the database spread over observing seasons during 2010–2013, comprising of the quality-assured and well-calibrated MICROTOPS II Sun Photometer measured AODs were used in conjunction with the trajectory classification scheme and hence for the characterization of the aerosols over the site. The data were analyzed both collectively and on seasonal basis to discern dominant aerosol types in winter and pre-monsoon season over the study site.

2. Study location and local meteorology

Pune (18°32′N, 73°51′E, 559 m amsl) is a rapidly growing city in terms of industrial installations, vehicular population and urbanization due to the boom in housing industry since the last two decades. It is situated on the leeside of the Western Ghats and is about 100 km inland from the west coast of India.

The environment in the immediate vicinity of the station is urban, with several small industries nearby and the possible aerosol type present over the station is a mixture of water soluble, dust-like and soot-like aerosols (Khemani, 1989). Formation of aerosols in the accumulation-mode is considered to be due to gas-to-particle conversion processes, whereas coarse-mode aerosols are attributed mainly to windblown dust (Khemani et al., 1982). The weather at the experimental site during the pre-monsoon season (March–May) is very hot with mostly gusty surface winds and the daytime maximum temperature reaching around 40 °C. Fig. 1(a, b) shows wind rose diagram constructed for forenoon (FN) and afternoon (AN) during observing season from December 2010 to May 2012 at the observing site, Pune as an example. From the figure is seen that in pre-monsoon, winds are predominantly north-westerly with speed up to 1–11 knots during FN and 1–17 knot during AN percentage of calm wind being 13.43 (AN) and 7.53 (FN). During this season, the dust content in the atmosphere is at a maximum, and cumulonimbus type cloud development takes place around late afternoon to evening (Khemani et al., 1982; Khemani, 1989). Development of low-pressure system due to increased heating over land starts over India in the pre-monsoon, when pressure distribution all over India is the same. The air flow in the lower troposphere is predominantly westerly during the south-west (SW) monsoon season (June–September), which brings a large influx of moist air from the Arabian Sea. The region receives light, continuous or intermittent rain, and the atmosphere is relatively free from dust during this season. The westerly flow sets in during the post-monsoon season (October–November). The continental air-masses, rich in nuclei of continental origin, pass over the region during this season.

The daily minimum temperature falls very rapidly by the end of October. Fair-weather conditions, with clear skies and very low relative humidity, exist during the winter (December–February) season. Low level capped inversions during the morning and evening hours, and dust haze during the morning hours, occur during this season (Devara et al., 1994; Aher et al., 2000; Pandithurai et al., 2007; Pawar et al., 2012). Fig. 1(c, d) shows a wind rose diagram constructed for forenoon (FN) and afternoon (AN) during observing season December 2010 to May 2012 at the observing site, Pune. From the figure it can be seen that in winter, winds are predominantly northeasterly with speed up to 1–11 knots during both FN and AN with percentage of calm wind being in the range of 5.22 (AN) and 21.21 (FN).

The city, thus receives both marine (due to westerly winds from the Arabian Sea) as well as continental (due to easterlies from adjoining land part) air-masses in one annual cycle. Due to the variety of the regions around Pune, different classes of particles can be found over its atmosphere: desert dust, originated from the Sahara desert, from arid regions in the Arabia and Thar Desert; polluted particles, produced mainly in urban and industrial areas of Indo-Gangetic Basin (IGB); marine aerosol, formed over the Bay of Bengal (BoB), Arabian or transported from the Indian Ocean; and biomass burning particles, often produced in forest fires, mainly during the pre-monsoon.

3. Data and methodology

To study the impact of long range transport of aerosols on the growth and decay of AOD at Pune and also to back trace the source and path of aerosol transport for all the days, we made use of AOD data obtained by operating MICROTOPS II Sun Photometer from the campus of the Nowrosjee Wadia College (NWC), Pune (India) on clear sky, cloudless observing days at multiple wavelengths during 2010–13 and the HYSPLIT model derived 5-day back-trajectories (Draxler and Hess, 1988). The five-day period was considered in view of the typical residence time of 1 week for aerosol in the lower troposphere (Ramanathan et al., 2001; Dubovik et al., 2008). As the AOD values are caused by the columnar aerosols, we considered three height levels representing the topography of the observation site viz., 500 m (within Atmospheric Boundary Layer, ABL), 1500 m (above ABL) and 4000 m (in the lower free troposphere) (Moorthy et al., 2003; Kaskaoutis et al., 2009). Also, in order to establish AOD climatology over Pune we use the last ten year (2004–2013) record of aerosol optical depth at 550 nm obtained from the MODIS instrument onboard the NASA EOS

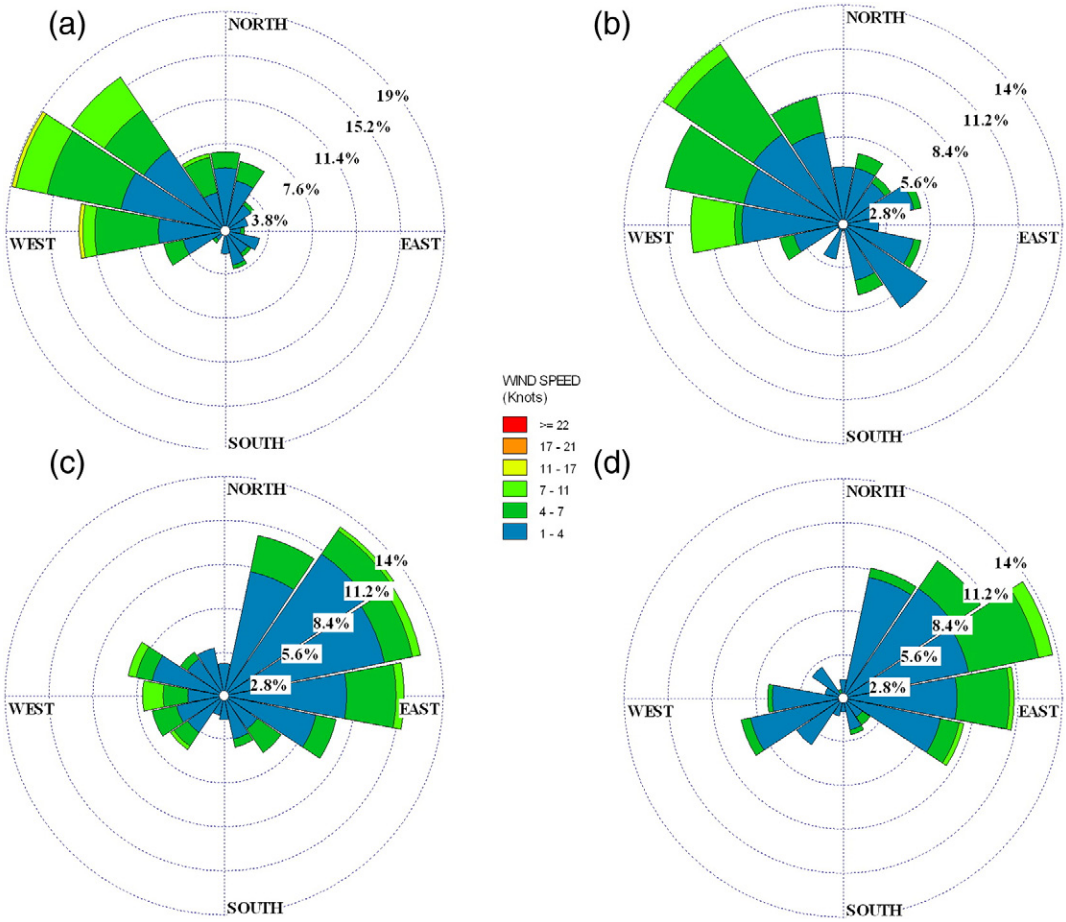

Fig. 1. Wind rose observed over Nowrosjee Wadia College, Pune (a) winter (FN), (b) winter (AN), Pune (c) pre-monsoon (FN), and (d) pre-monsoon (AN) during 2010–12.

Terra satellite. This is supplemented with AERONET AOD data at 500 nm during 2008–2013.

3.1. MODIS and AERONET data

MODIS (Moderate-resolution Imaging Spectroradiometer) instrument makes radiance observations in 36 spectral channels at spatial resolution ranging from 250 m to 1 km with a 2300 km wide swath, allowing for almost daily global coverage. We use a level 3 gridded product used recently in a number of studies (Kosmopoulos et al., 2008; Kanakidou et al., 2011; Alam et al., 2011a,b; Kharol et al., 2011). MODIS land aerosol algorithm makes use of the so-called dark target approach (Levy et al., 2010). AERONET (Aerosol Robotic NETwork) AOD is derived from direct sun Photometer measurements in certain or all of the following seven various spectral bands centered at 340, 380, 440, 500, 670, 940 and 1020 nm. AERONET measures the extinction of direct beam solar radiation and applies the Beer–Lambert–Bouguer law to determine AOD (Holben et al., 1998) with uncertainties of the order of 0.01–0.02 (Eck et al., 1999). Only cloud-screened and quality assured AERONET Level 2 AOD data at 500 nm wavelength data are used in this study (Smirnov et al., 2000).

3.2. Measurement of aerosol optical depth

A microprocessor-controlled MICROTOPS-II Sun Photometer (manufactured by Solar Light Company, USA) was operated to measure AOD at five wavelengths, viz., 440, 500, 675, 870 and 1020 nm. The full width at half maximum (FWHM) bandwidth for all channels is 10 ± 1.5 nm. MICROTOPS-II Sun Photometer has built-in pressure and temperature sensors with GPS connectivity to obtain the position and time coordinates of the observing site. The measurement protocol is based upon the principal of measuring the intensity of incoming solar radiation at the particular wavelength and, then converting it into optical depth using its internal calibration employing Langley method. The irradiance signal (in mV) at different wavelengths is multiplied with the calibration factor (in W/m^2 mV) and the absolute irradiance is obtained in W/m^2. It is found that the error in calibration of the Sun Photometer ($I_{0,\lambda}$) is $<\pm 0.5\%$ for measurements at different wavelengths for air-mass value of one (for overhead sun), which yields ~0.005–0.03 error in optical depth. At larger air-mass, the errors in AOD decrease. Overall error in AOD measurements is found to be ± 0.03 (Devara et al., 2001; Pawar et al., 2012). The Sun photometric observations were systematically performed at the Nowrosjee Wadia College, Pune (India) under clear and cloudless conditions from morning till evening during 2010–13. AOD data of about four hundred observing days comprising of sixteen thousand AOD spectra was used in the present study.

3.3. Estimation of Ångström parameters, α and β

The dependence of AOD on wavelength provides valuable information about physical properties of aerosols. These can be derived from Ångström empirical formula as (Ångström, 1961),

$$\tau_{p\lambda} = \beta\,\lambda^{-\alpha} \tag{1}$$

where, Ångström exponent (AE, α) is an indicator of fraction of accumulation-mode aerosols (radii < 1 μm) to coarse-mode aerosols (radii > 1 μm). β, Ångström turbidity coefficient (which equals $\tau_{p\lambda}$ at 1000 nm), is a measure of columnar aerosol loading. Values of both α and β are determined by evolving linear least squares fit between $\tau_{p\lambda}$

and λ (in μm) on log–log scale over the spectral range of MICROTOPS II Sun Photometer. The slope and intercept of the regression line yield α and ln β respectively.

3.4. Trajectory classification scheme

Each computed trajectory is associated with corresponding aerosol optical characteristics. However, relating column integrated quantities to trajectories at specific altitudes may be problematic and may not give a clear indication of the dominant aerosol type. It was found that the definition of the sector might be proportionally different to the air-mass altitude used. Therefore, great differences in the aerosol origin may be revealed if the analysis is based on back-trajectories in the boundary layer (500 m and 1500 m) or in the free troposphere (4000 m). Investigation of this aspect constitutes the main goal of the present study. Considering main advection patterns over Pune, five

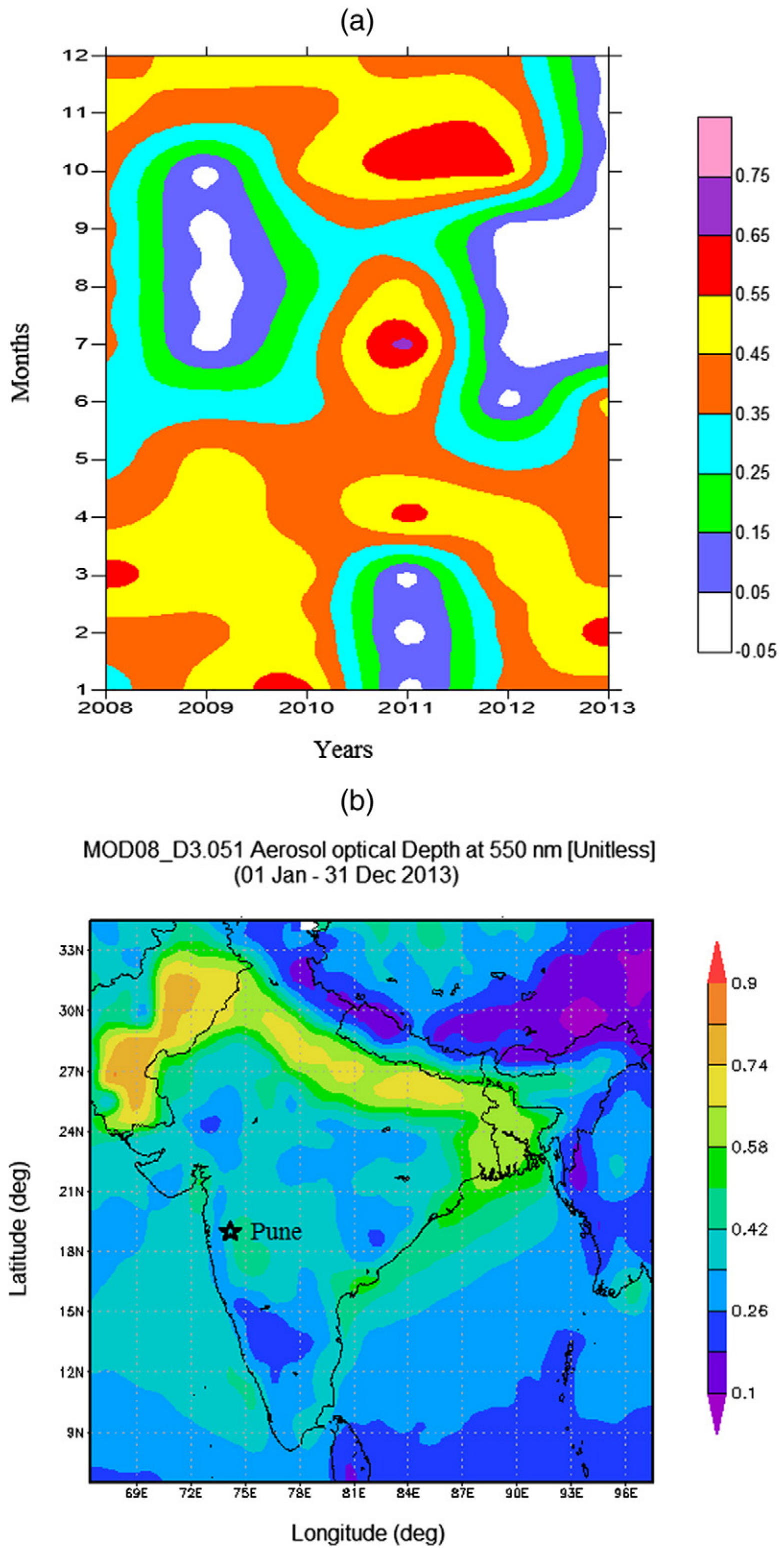

Fig. 2. (a) A 2-D Contour diagram of AERONET retrieved $AOD_{500\ nm}$ during 2008–2013. (b) Spatial climatology of MODIS (Terra) measured $AOD_{550\ nm}$ during 2004–2013.

geographical sectors were defined in relation to different aerosol sources. The main pathways/sectors revealed from trajectory analysis are the following:

a) A Northwestern, North sector (NW/W), including North African countries, Sahara Desert, Arabian Desert, Gulf countries and North Indian region including Thar Desert is expected to contribute aerosols of desert-dust in origin.
b) A Southwestern, South sector (SW/S), which includes the South Arabian Sea and North Indian Ocean is supposed to be of marine type.
c) A North sector (N), including Indo-Gangetic Basin (IGB) region, r-epresents dominant aerosols of anthropogenic origin.
d) A Southeastern, Eastern sector (SE/E), associated with the Bay of Bengal (BoB), including industries along the coastal areas of BOB denotes aerosols comprising a mixture of marine along with anthropogenic origin.
e) A local sector (L) including continental Pune, Deccan plateau region, represents dominant aerosol type of local emissions (mainly anthropogenic) i.e., urban/industrial aerosols.

The back-trajectory classification scheme used here is based on the residence time of a particular trajectory within a pre-defined region. The time spent by the trajectory in a sector up to the measurement day at the observing site was considered to better define the corresponding aerosol origin sector. Trajectories were assigned to a particular sector if they resided over it for more than 80% of their travel time before arriving the experimental site (diSarra et al., 2001; Formenti et al., 2001; Gerasopoulos et al., 2003; Gogoi et al., 2008; Santese et al., 2008). On the basis of this classification scheme, we define trajectories to represent each of the five air-mass types described above and use them to identify various aerosol types.

However, a degree of arbitration in the definition of the sectors may exist due to the effective distribution of the sources. Nevertheless, a little change in the boundaries of the sectors does not significantly affect the results on the climatological basis (Pace et al., 2006; Kaskaoutis et al., 2009). Also, the use of different back-trajectories with varying duration (either 3 or 7 days) does not significantly modify the average aerosol optical properties in each sector. Therefore, the simple trajectory classification scheme used in the present work appears to be sufficiently capable to allow the identification of the main aerosol types.

4. Results and discussion

4.1. Climatology of aerosol optical depth

In this section we present the long-term climatology of aerosol optical depth measured from both the ground (AERONET)- and satellite (MODIS)-based sensors over the observing site Pune. The results are shown in Fig. 2(a) and (b) respectively.

The monthly mean AOD data at 500 nm, a mid-visible wavelength, retrieved from the AERONET measurements at Pune have been averaged over 2008–2013 periods. Results shown in Fig. 2(a), reveals the temporal variability of measured $AOD_{500\ nm}$ in the form of a 2-D contour diagram. At the outset, AODs exhibit strong seasonal variation. This

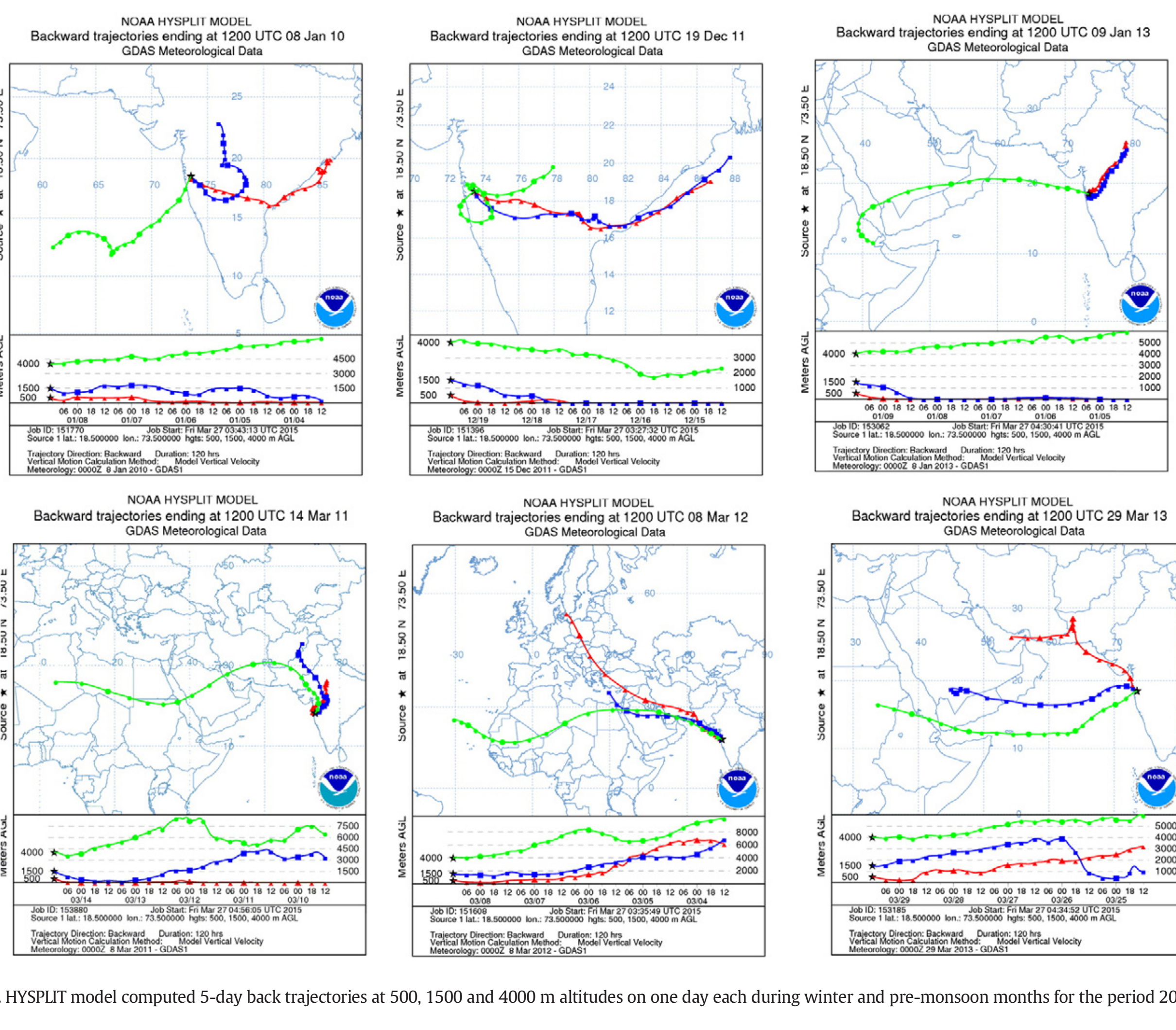

Fig. 3. HYSPLIT model computed 5-day back trajectories at 500, 1500 and 4000 m altitudes on one day each during winter and pre-monsoon months for the period 2010–13.

regular nature of annul/seasonal variations of AOD would be due to the influence of perturbing factors which are regular in nature, at least on regional scale. As the observing site is significantly influenced by industrial and urban activities, the regular variations in AODs are indicative of both natural and anthropogenic processes, having a regular annual cycle, which modify the optical depths through combination of production, transport and removal mechanisms of regional importance. The strong pre-monsoon surface winds enhance the production of continental aerosols from dry land surfaces. Increased convective activity during pre-monsoon months and gas-to-particle conversion by photochemical reactions also contribute to this (Moorthy et al., 1999, 2013; Kumar et al., 2012; Babu et al., 2013).

Fig. 2(b) shows the spatial climatology of MODIS Terra measured yearly mean $AOD_{550\ nm}$ over the Indian subcontinent for the period 2004–13. From the figure, it is seen that the Indo-Gangetic Basin (IGB) in the northern part of India shows a sharp contrast in MODIS derived AODs in the range 0.58–0.74. As compared to southern India and especially Pune, the observing site of the present study, AODs over IGB region are significantly high. The reason for high AODs over the IGB region is the large influx of desert dusts from the western arid and desert regions of Arabia, Africa and Thar (Rajasthan) regions during the pre-monsoon season (April–June) in addition to the dense population, heavy industries (Dey et al., 2004; El-Askary et al., 2004, 2006; Singh et al., 2005; Gautam et al., 2009a,b). Moreover, over the entire Indian region, there is large gradient in AOD increase from South to North (Prasad et al., 2004).

4.2. Main sectors for the occurrence of each aerosol type

In this section, we retrieved 5-day HYSPLIT air-mass back trajectories for individual day of observation during 2010–2013. Fig. 3 shows examples of map of one day each during winter and pre-monsoon months for the entire period of observation. Using air-mass trajectories for each observing day, we developed a climatological description of air-mass types based on of their frequency of occurrence and seasonal distribution falling into the appropriate sector. The result of this analysis is shown in Fig. 4(a) and (b) which depict the frequency of occurrence of air-mass types at 500, 1500 and 4000 m altitude levels falling in each sector and arriving at Pune in the winter (December–February) and pre-monsoon (March–May) seasons, for all the days during the three observing seasons during the years 2010–2013. For determination of the frequency distribution, all possible days during study period are considered so as to avoid any statistical bias that might result if the MICROTOPS II Sun Photometer measurements were not evenly distributed throughout the period.

From Fig. 4(a), it is seen that during winter at Pune, the aerosol influx may be pre-dominantly from the SE/E and N sectors at lower (500 m) and mid (1500 m) altitude levels as revealed by the average occurrence of air-mass trajectories of about 60% and 35% respectively, arriving from Bay of Bengal and Northern India. A combined occurrence of SE/E and N sector air-masses ranges from 60% at 500 m to 53% at 1500 m in winter. The air-masses in the free troposphere (i.e. around 4000 m altitude) are found to have smaller signatures in the SE/E sector while in the L sector their presence is minimal and their presence in the N sector is totally absent. Thus, it is clear that during winter, the SE/E and N sectors are favored by air-masses within or above atmospheric boundary layer enabling study of aerosol properties from the trajectories at 500 and 1500 m altitudes. Similar studies (Gautam et al., 2007; Das et al., 2008) reveal that the air-masses at lower altitudes arrive from the IGB and BoB where intense fog and pollution-haze conditions occur during early morning hours in winter season. This airmass transport may carry anthropogenic aerosols and pollutants to the observing site, Pune, resulting in higher abundance of sub-micron aerosols mixed with natural aerosols.

Air-mass trajectories within the SW/S sector at 500 m altitude are almost absent during winter over Pune while 24% of observed air masses arriving from the NW/W sector, 23% from the Middle East and 1% from the Arabian Sea are driven by the Western synoptic circulation pattern in Northern mid-latitudes (Sinha et al., 2012). Since these air-masses traverse over the desert/arid regions of Arabia, Pakistan, Iran and North Western India (mainly at 4000 m altitude) are normally found to carry significant amounts of dust-laden aerosols over the Arabian Sea and Continental India on certain occasions (Badarinath et al., 2010). However, the low frequency viz., 23% and 1% of occurrence of arid and marine air-masses in winter does not favor the considerable presence of coarse-mode aerosol particles and the dominance of fine-mode aerosols over Pune. The aerosol production mechanism related to wind and surface conditions is weak in winter season so that the transport of mineral dust is less significant (Aloysius et al., 2008).

During pre-monsoon season, contributions from NW/W as well as the SW/S air-mass sectors are considerable (Fig. 4b). Air-masses to the tune of about 53%, arriving at Pune, originate from West Asian Countries which are rich in coarse-mode aerosols as the dust activity over this region is at its maximum during the pre-monsoon (Gautam et al., 2009a,b, c; Aher et al., 2014). On the other hand, in several cases (~25%), the air-masses arriving from the Indian Ocean crossing the Arabian Sea before reaching Pune advect marine air-masses. However, on some occasions, air-masses from nearby or across some coastal parts of East Africa or Arabian coast bring continental air mixed with marine air. This leads to the enhanced aerosol loading constituting both fine- and coarse-mode aerosol particles (Safai et al., 2005). It is seen that, in the present case, for the NW/W sector, AODs and β values are higher whereas α values are lower indicating the presence of coarse-mode aerosols (Table 1).

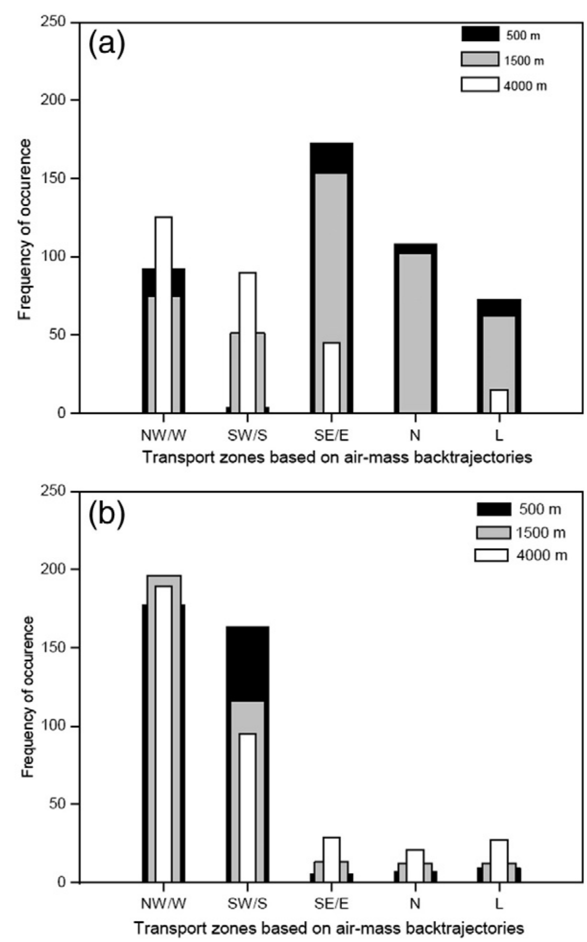

Fig. 4. (a): Percent contribution of different source regions to air-mass flow at 500, 1500 and 4000 m altitudes over Pune for winter season during 2010–13. (b): Same as in Fig. 3(a), but for pre-monsoon seasons during 2010–13.

Table 1
Classification of $AOD_{500\ nm}$, Ångström exponent (AE, α) and Ångström turbidity coefficient (β) with respect to different pathways/sectors and altitudes.

Season	Trajectory altitude	Group	Air-mass sectors	$AOD_{500\ nm}$ ($\tau_{p\lambda}$)	Ångström exponent (AE, α)	Ångström turbidity coefficient (β)	Number of occurrences
Winter	500 m	1	NW/W	0.48 ± 0.18	1.05 ± 0.11	0.20 ± 0.12	24
		2	SW/S	–	–	–	0
		3	SE/E	0.43 ± 0.03	1.19 ± 0.15	0.17 ± 0.07	81
		4	N	0.50 ± 0.05	1.14 ± 0.21	0.23 ± 0.06	64
		5	L	0.51 ± 0.11	1.14 ± 0.13	0.25 ± 0.07	40
	1500 m	1	NW/W	0.39 ± 0.09	1.10 ± 0.10	0.16 ± 0.04	30
		2	SW/S	0.50 ± 0.03	1.15 ± 0.23	0.26 ± 0.08	17
		3	SE/E	0.45 ± 0.10	1.18 ± 0.17	0.27 ± 0.06	78
		4	N	0.50 ± 0.08	1.15 ± 0.19	0.22 ± 0.07	40
		5	L	0.49 ± 0.15	1.14 ± 0.11	0.24 ± 0.06	38
	4000 m	1	NW/W	0.54 ± 0.15	1.16 ± 0.13	0.24 ± 0.10	105
		2	SW/S	0.54 ± 0.06	1.14 ± 0.22	0.25 ± 0.06	57
		3	SE/E	0.41 ± 0.01	1.18 ± 0.09	0.21 ± 0.01	19
		4	N				0
		5	L	0.45 ± 0.19	1.02 ± 0.11	0.23 ± 0.09	4
Pre-monsoon	500 m	1	NW/W	0.53 ± 0.15	0.77 ± 0.12	0.37 ± 0.12	75
		2	SW/S	0.35 ± 0.07	0.76 ± 0.17	0.33 ± 0.06	87
		3	SE/E				2
		4	N	0.51 ± 0.10	0.64 ± 0.13	0.36 ± 0.14	3
		5	L	0.52 ± 0.28	0.92 ± 0.15	0.34 ± 0.07	4
	1500 m	1	NW/W	0.57 ± 0.12	0.69 ± 0.08	0.33 ± 0.05	83
		2	SW/S	0.47 ± 0.08	0.79 ± 0.16	0.25 ± 0.06	65
		3	SE/E	0.41 ± 0.19	1.14 ± 0.04	0.29 ± 0.11	4
		4	N	0.60 ± 0.12	0.91 ± 0.05	0.27 ± 0.04	3
		5	L	0.56 ± 0.21	0.97 ± 0.11	0.30 ± 0.06	4
	4000 m	1	NW/W	0.61 ± 0.21	0.54 ± 0.14	0.32 ± 0.04	99
		2	SW/S	0.39 ± 0.08	0.75 ± 0.23	0.20 ± 0.09	45
		3	SE/E	0.49 ± 0.27	0.98 ± 0.25	0.25 ± 0.10	19
		4	N				
		5	L	0.60 ± 0.29	0.78 ± 0.20	0.30 ± 0.07	5

4.3. Classification of aerosol properties based on transport pathways

The spectral AODs of each observation day were assigned to each of the sectors by adopting the classification scheme described in Section 3.3 required. From each AOD spectra so classified, α and β values were estimated by implementing the method outlined in Section 3.2. These values were averaged for each trajectory group. The results are presented in Table 1 which compiles sector wise mean values and corresponding standard deviations of various aerosol optical parameters viz., $AOD_{500\ nm}$ AE (α) and β over Pune for winter and pre-monsoon seasons during 2010–2013.

Table 1, illustrates the role of lower and middle altitude air masses originating from the North sector (mainly IGB region) in carrying a significant amount of aerosols over the study region accounting for the observed high AODs in the range 0.50 ± 0.05 (at 500 m) to 0.60 ± 0.12 (at 1500 m) with corresponding AEs in the range 1.14 ± 0.21 to 0.91 ± 0.05 during winter and pre-monsoon seasons respectively. The plausible reason for this observation may be the winds carrying continental air-masses from North Indian regions, through IGB, further crossing the central Indian region, or sometimes from Eastern coastal regions crossing through the central part of India and then arrive at Pune. It is clear from the above discussion that easterly winds which arrive from Northeast Indian regions (covering IGB and central Indian regions) produce influx of polluted fine-mode aerosols at the observing site (Safai et al., 2005).

In the pre-monsoon season, air-masses from the NW/W and SW/S sectors are mainly dominant over the site as is revealed in Fig. 4(b). The desert dust is well identified from the trajectory analysis, and corresponds respectively to the NW/W sector. As expected, aerosols from this sector have the largest average AOD ($\tau_{p\lambda} = 0.61 \pm 0.21$), and the lowest AE ($\alpha = 0.54 \pm 0.14$). The values of AOD and columnar loading β are the highest during this period when the trajectories originate in the NW/W sector. Thus, the highest value of β in the pre-monsoon season indicates an increase in the loading of coarse-mode particles till the onset of monsoon. An increase in AOD values (from 0.53 to 0.61) from the NW/W sector is observed as the air-mass altitude increases. This suggests that the dust transport over Pune occurs mainly in the free troposphere. During the pre-monsoon season, sector SW/S also contributes to AOD enhancement over Pune. As expected, the air-masses from this sector at all altitudes are lower because of the transport of marine aerosols from the Arabian Sea and the Indian Ocean (Table 1). Another interesting feature is the very high AOD value ($\tau_p = 0.60 \pm 0.29$), despite the limited number of cases corresponding to air-masses at 4000 m from sector L. The large standard deviations also confirm that these values are not representative for the whole dataset. There is a rapid build-up of in the AODs over the site after March, as the arid air-mass type is known to transport large amount of desert and mineral aerosols from the West Asian and Indian Desert area. Also, influx of aerosols (mostly coarser fraction) from Thar Desert and dry season during pre-monsoon causes high AOD over Pune. Thus, from the above discussion it is clear that the aerosol layers above the atmospheric boundary layer are normally transported from distances of the order of thousands of kilometers and can contribute significantly to the columnar AOD variations (Franke et al., 2003; Lin et al., 2007; Xu et al., 2009).

4.4. Frequency distribution of AOD and Ångström exponent

In this section, histograms are displayed for the five different air-mass sectors described in Section 4.1 (Fig. 4a and b). To determine the frequency distribution, we considered all AODs at 500 nm wavelength and the corresponding Ångström exponents categorized for 1500 m altitude. The 1500 m level is chosen because of the larger errors affecting the concerned AOD data at the 500 m level and diminished aerosol load at 4000 m level, except in some cases involving desert dust air masses (Toledano, 2005).

As seen from the frequency plot (Fig. 5a), for the NW/W sector air-masses, $AOD_{500\ nm}$ lies between 0.3 and 0.7 in 92% of all cases, with a peak frequency occurring at 0.5. The corresponding histogram of Ångström exponent for the arid air mass (Fig. 5b) shows a primary peak at 0.5, secondary peak at 0.9 and a range from 0.1 to 1.4. The SW/S sector

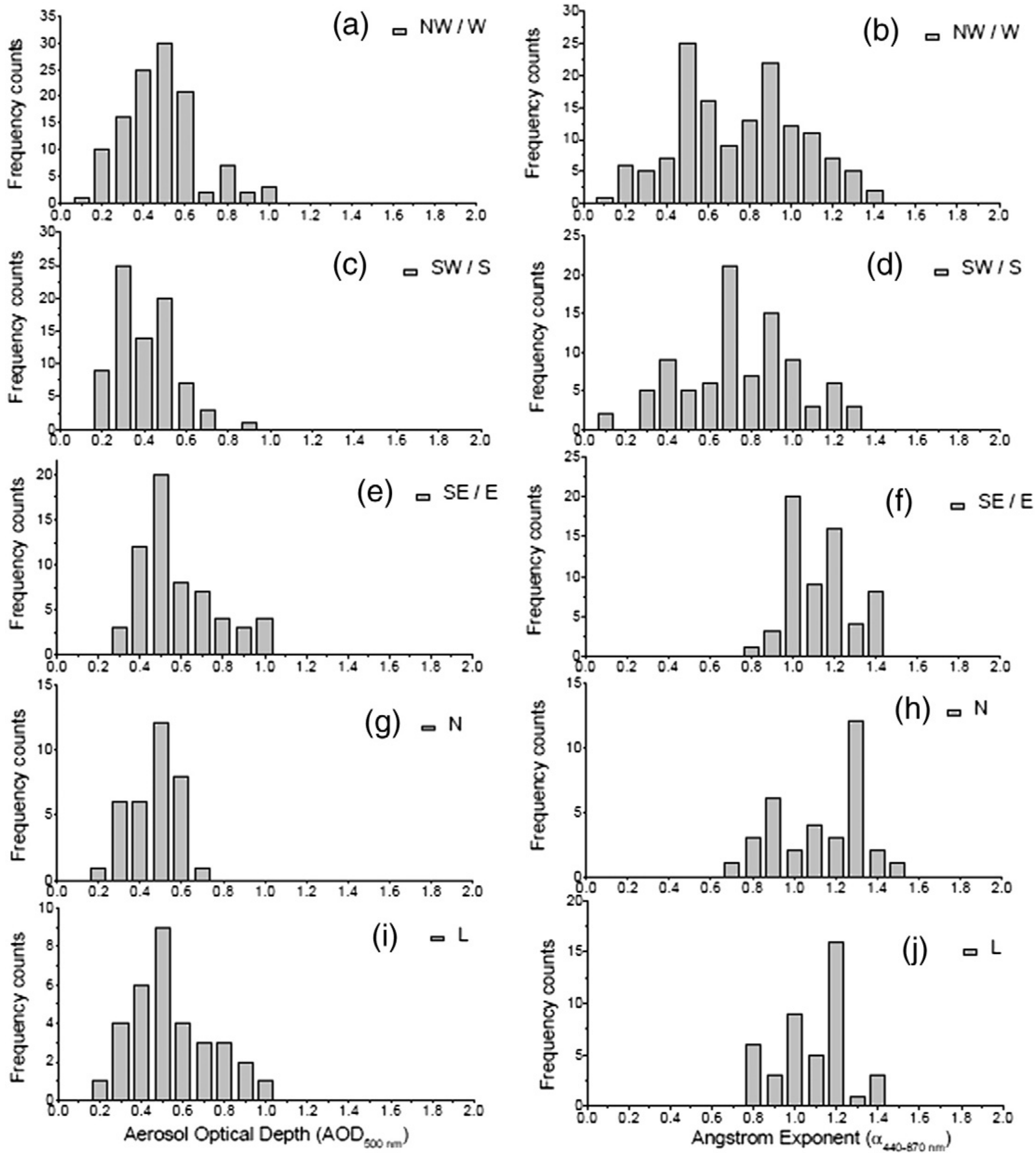

Fig. 5. Frequency distribution of AOD (left) and AE (right) for the cases at 1500 m altitude.

air masses (Fig. 5c) generally tend to have lower $AOD_{500\ nm}$ values (<0.5; 81% of occurrences) with corresponding Ångström exponent having peak at 0.7 and range from 0.1 to 1.4. Fig. 5d shows that the frequency of occurrence for the SW/S sector air masses is of bimodal type with peak frequencies at AE values of 0.4 and 0.5. This clearly indicates the influence of the mixed type of aerosols consisting of coarse (Sea salt) and fine-mode (anthropogenic) aerosols from the industrialized areas of the Indian West coast, which has a spatial offshore extent of <100 km at the coast (Moorthy et al., 2008). Also, in several cases, the air-masses arriving at the present observing site from the Indian Ocean traversing over Indian Peninsular region usually carry aerosols from biomass-burning as a result of the crop residue burning during March–May period. This leads to enhanced aerosol loading constituting both fine- and coarse-mode particles (Sinha et al., 2012).

The frequency histogram of AOD for the air-masses advected from SE/E sector (Fig. 5e) has the AOD peak value at 0.5 and related peak AE (Fig. 5f) value at 1.0 with a span of 0.8–1.4, clearly indicating the presence of sub-micron/accumulation-mode particles traveling from the BoB and continental Indian landmass to the present observing site. Northern sector air-masses (Fig. 5g) have an optical depth (ranging from 0.3 to 0.6) and AE between 0.8 and 1.4 (Fig. 5h); these values are consistent with those of the anthropogenic aerosols, as expected for highly polluted region of IGB (Badarinath et al., 2008). The L air masses (Fig. 5i) also have a broad size range of AOD i.e. 0.2–1.0 and corresponding AE having a peak at 1.2 and a range of 0.8–1.4 (Fig. 5j). The range of both AOD and AE for sectors SE/E and L is very similar. Dani et al. (2012) reported that over Pune, both size exponent viz., AE (α) and turbidity coefficient (β) have increased steadily at the rate of 25.3 and 8.4% per decade, respectively. The steady increase in AE over the 10-year study period clearly points out that over the years due to increasing urbanization and human activities, more and more fine-mode sized aerosols are being added to the ambient atmosphere. Thus, the analysis of frequency histograms within each sector reveals important features about the different aerosol types.

4.5. Scatter plot of AE–AOD and discrimination of different aerosol types

Fig. 6a and b shows the sector wise scatter plots of AE against $AOD_{500\ nm}$ during winter and pre-monsoon seasons separately for the period 2010–2013 enabling classification of different aerosol types

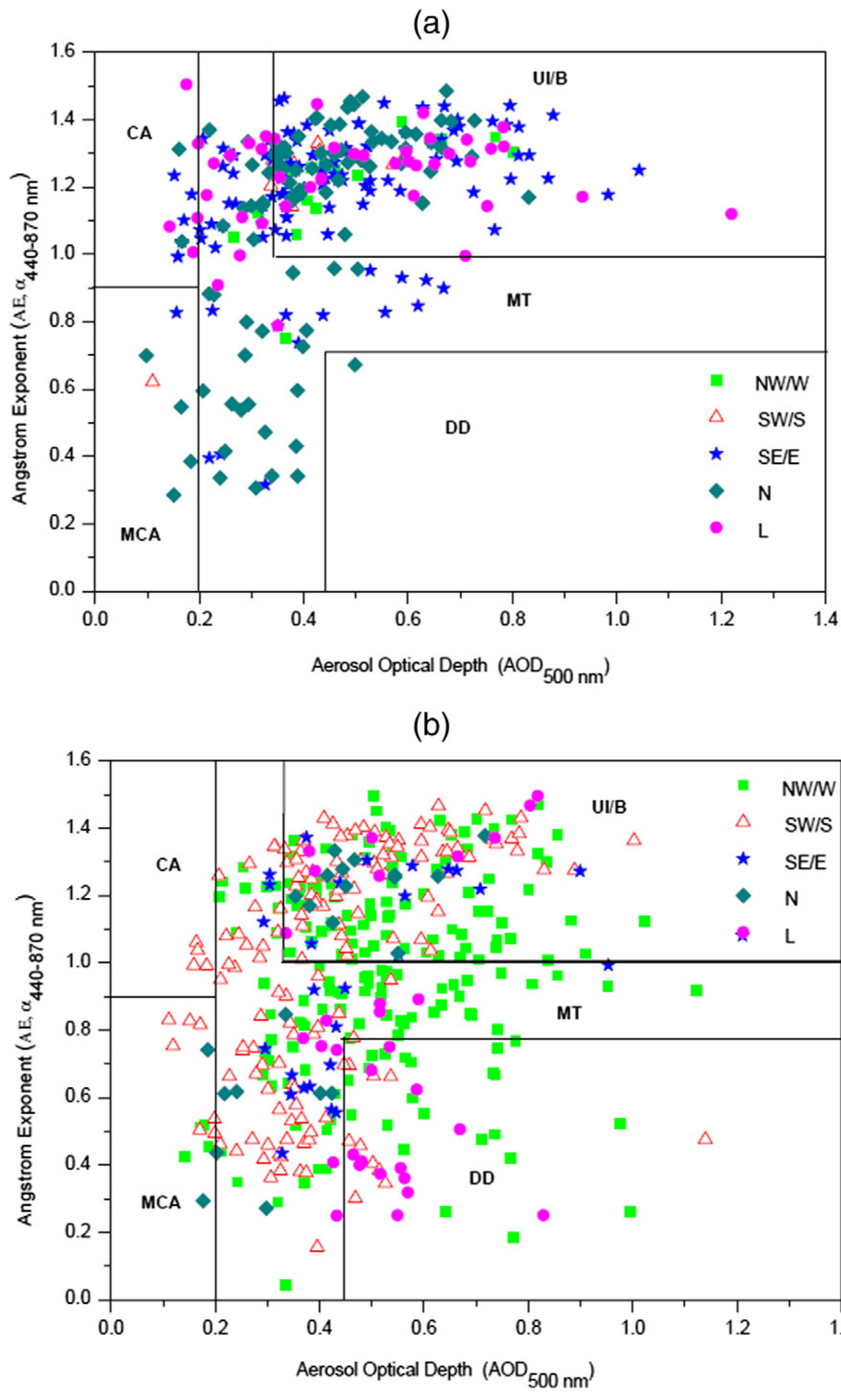

Fig. 6. (a, b). Scatter plot of AE Versus AOD (daily means) according to the classification scheme.

hovering over Pune. The method is based on the sensitivity of these two parameters to different, somewhat independent, microphysical aerosol properties. Experimental evidence reveals that $AOD_{500\ nm}$ depends on the aerosol columnar density and size while Ångström exponent depends on the size of particles (Kaskaoutis et al., 2009).

The discrimination of aerosol types (Table 2) is generally achieved by means of widely used method of relating aerosol load (i.e. $AOD_{500\ nm}$) and particle size (i.e. α) used by several investigators (Eck et al., 1999; Pace et al., 2006; Kaskaoutis et al., 2007a,b,c, 2009, 2011; Kalapureddy et al., 2009; Pathak et al., 2012; Sharma et al., 2014; Vijayakumar et al., 2014). By assuming a variety of $AOD_{500\ nm}$ values and α in the spectral range 340–1020 nm over AERONET location in Bahrain, Eck et al. (1999) have identified three distinct aerosol types viz., biomass burning, urban/industrial and desert dust. Pace et al. (2006) made a distinction between desert dust and biomass burning/urban aerosols over Lampedusa at Central Mediterranean Sea and considered the remaining aerosols as mixed aerosols. A similar study over four AERONET stations at Alta Floresta (Brasil), Ispra (Italy), Nauru (Pacific Ocean) and Solar Village (Saudi Arabia) treated clean maritime aerosols as the background aerosols and further distinguished other aerosol types as desert dust, biomass burning, urban/industrial and mixed aerosols (Kaskaoutis et al., 2007b). In the Indian subcontinent, Kaskaoutis et al. (2009) have distinguished different aerosol types originating from variety of sources over Hyderabad. Further, Kalapureddy et al. (2009) over the Arabian Sea and Kaskaoutis et al. (2011) over BoB have discriminated different aerosol types over

Table 2
Optical properties of different aerosol types at environmentally different locations.

Location	$AOD_{500\ nm}$	AE	Types of aerosol	Reference
Bahrain	0.41	$\alpha_{340–1020} = 1$	Desert dust	Eck et al. (1999)
Lampedusa	$AOD_{495.7} \geq 0.15$	$\alpha_{415.6–868.7} \leq 0.5$	Desert dust	Pace et al. (2006)
	$AOD_{495.7} \geq 0.1$	$\alpha_{415.6–868.7} \geq 1.5$	Biomass burning/urban	
	Remaining	Remaining	Mixed	
Nauru	<0.06	$\alpha_{440–870} < 1.3$	Clean maritime	Kaskaoutis et al. (2007b)
Alta	>1	$\alpha_{440–870} > 1.5$	Biomass burning/urban	
Floresta and Ispra			Industrial	
Solar village	>0.15	$\alpha_{440–870} < 0.5$	Desert dust	
	0 to ~1.5	$\alpha_{440–870}$ −0.5~1.5	Mixed	
	<0.15	$\alpha_{340–1020} < 1.3$	Clean maritime	
Arabian	>0.2	$\alpha_{340–1020} > 1$	Urban industrial	Kalapureddy et al. (2009)/
	>0.25	$\alpha_{340–1020} < 0.7$	Desert dust	Kaskaoutis et al. (2011)
	Remaining	Remaining	Mixed	
Hyderabad	<0.3	$\alpha_{380–870} < 0.9$	Clean maritime	Kaskaoutis et al. (2009)
	>0.5	$\alpha_{380–870} < 1$	Urban/industrial	
	>0.6	$\alpha_{380–870} < 0.7$	Desert dust	
	Remaining	Remaining	Mixed	
Dibrugarh	<0.2	$\alpha_{380–1025} < 1.4$	Continental average	Pathak et al. (2012)
	<0.2	$\alpha_{380–1025} < 0.9$	Marine continental average	
	>0.35	$\alpha_{380–1025} > 1$	Urban/biomass burning	
	>0.45	$\alpha_{380–1025} < 0.7$	Desert dust	
	Remaining	Remaining	Mixed	
Pune	<0.2	$\alpha_{440–870} < 1.6$	Continental average	Present study
	<0.2	$\alpha_{440–870} < 0.9$	Marine continental average	
	>0.35	$\alpha_{440–870} > 1$	Urban/biomass burning	
	>0.45	$\alpha_{440–870} < 0.7$	Desert dust	
	Remaining	Remaining	Mixed	

Oceanic regions surrounding the Indian landmass. Also, Pathak et al. (2012) at a rural observing site Dibrugarh situated on the Southern bank of river Brahmaputra in Eastern Assam, close to the North-Eastern boundary of the Indian subcontinent classified aerosols into five main types such as continental average (CA), marine continental average (MCA), urban/industrial and biomass burning (UI/B), desert dust (DD) and the remaining cases as indeterminate or mixed type (MT).

In the present work for defining the background aerosol type viz., the continental average (CA) type at the present study location which represents an urban continental environment influenced by human activities, a model given by Hess et al. (1998) has been used. According to this aerosol model, the magnitude of $AOD_{550\ nm}$ is 0.151 for background aerosols and AE in the spectral range 350–500 nm is 1.11 while in the range 500–800 nm, it is 1.42 at relative humidity (RH) of 80%. As seen from back-trajectory analysis, discussed above, and as the location is affected by advection from the Arabian Sea and BoB, the marine continental average (MCA) aerosol type is also assumed to be present as additional background aerosols. The threshold values for these types are taken as $AOD_{500\ nm} < 0.2$; $\alpha < 1.4$ for CA and $AOD_{500\ nm} < 0.2$; $\alpha < 0.9$ for MCA. Aerosols produced from local sources, transported biomass burning and of anthropogenic origin are termed as urban/industrial and biomass burning (UI/B) type. The dust or the minerals originated by the action of wind, particularly in western deserts including the coarse-mode aerosols under high RH conditions are termed as desert dust aerosols (DD). These two types are discriminated by adopting considerations employed by Kalapureddy et al. (2009) over the Arabian Sea, Kaskaoutis et al. (2009) over Hyderabad and Kaskaoutis et al. (2011) over BoB as the source regions for long-range transported aerosols over respective locations. The remaining aerosols which do not fall in any of the above categories are considered as undetermined or mixed type (MT) (Pace et al., 2006).

The scatterogram of AE versus $AOD_{500\ nm}$ constructed for the present data (Fig. 6a and b) forms physically interpretable individual sector wise cluster regions separated by the solid lines, each corresponding to different aerosol types. Within each cluster, however, large dispersion has been observed in terms of $AOD_{500\ nm}$ and AE. For example, AE varies over a wide range at low $AOD_{500\ nm}$ (<0.2) for CA as well as for MCA types during winter (Fig. 6a) and pre-monsoon (Fig. 6b) seasons. The increase in AE with increasing $AOD_{500\ nm}$ indicates the presence of fine mode aerosols in the atmospheric column. Significant numbers of points are accumulated in the cluster region $AOD_{500\ nm} > 0.35$, $\alpha > 1$, corresponding to the aerosol particles of UI/B type for both winter and pre-monsoon seasons. A less dense area with higher $AOD_{500\ nm}$ (>0.40) and $\alpha < 0.7$ indicates the presence of DD aerosols during pre-monsoon while their presence during winter is insignificant. The rest of the points are scattered corresponding to a variety of $AOD_{500\ nm}$ values ranging from ~0.2 to ~1.3 and a wide range of AE values (~0 to ~1.6). These points together with highly dense area with $0.2 < AOD_{500\ nm} < 0.45$, and $0.5 < \alpha < 1$ are difficult to be included in a specific cluster region like other aerosol types and hence are categorized as the MT aerosols bearing in mind the different effects of various aerosol-mixing processes in the atmosphere (e.g., coagulation, condensation, humidification, gas-to-particle conversion).

From Fig. 6a and b, it is seen that the MT aerosols are more prominent in pre-monsoon as compared to winter season. A mixed or indeterminate aerosol type is formed because of the complex combination of natural and anthropogenic factors (including RH, fuel types and emission characteristics) that influence aerosol formation and evolution (Kaskaoutis et al., 2009).

4.6. Seasonal heterogeneity in aerosol types

Fig. 7 shows the percent contribution of different aerosol types based on the present $AOD_{500\ nm}$ and $\alpha_{480–870\ nm}$ threshold values over Pune. The contribution of aerosols of different origin and characteristics to the atmospheric column can be strongly modified in each season. Thus, during the observing seasons for the period 2010–2013, UI/B aerosols are pre-dominantly observed in the range of 61–70% during winter season and 30–50% of MT type during pre-monsoon season.

The dominance of UI/B type in the winter season for all the years (i.e. 2010–2013) may be attributed to both local and transported aerosols. The former is revealed by confinement of 50% of trajectories below local atmospheric boundary layer, while the latter is evident from the trajectories at higher levels, which are mostly the SE/E and N sectors (i.e. BOB and IGB region). Vijayakumar et al. (2012) and

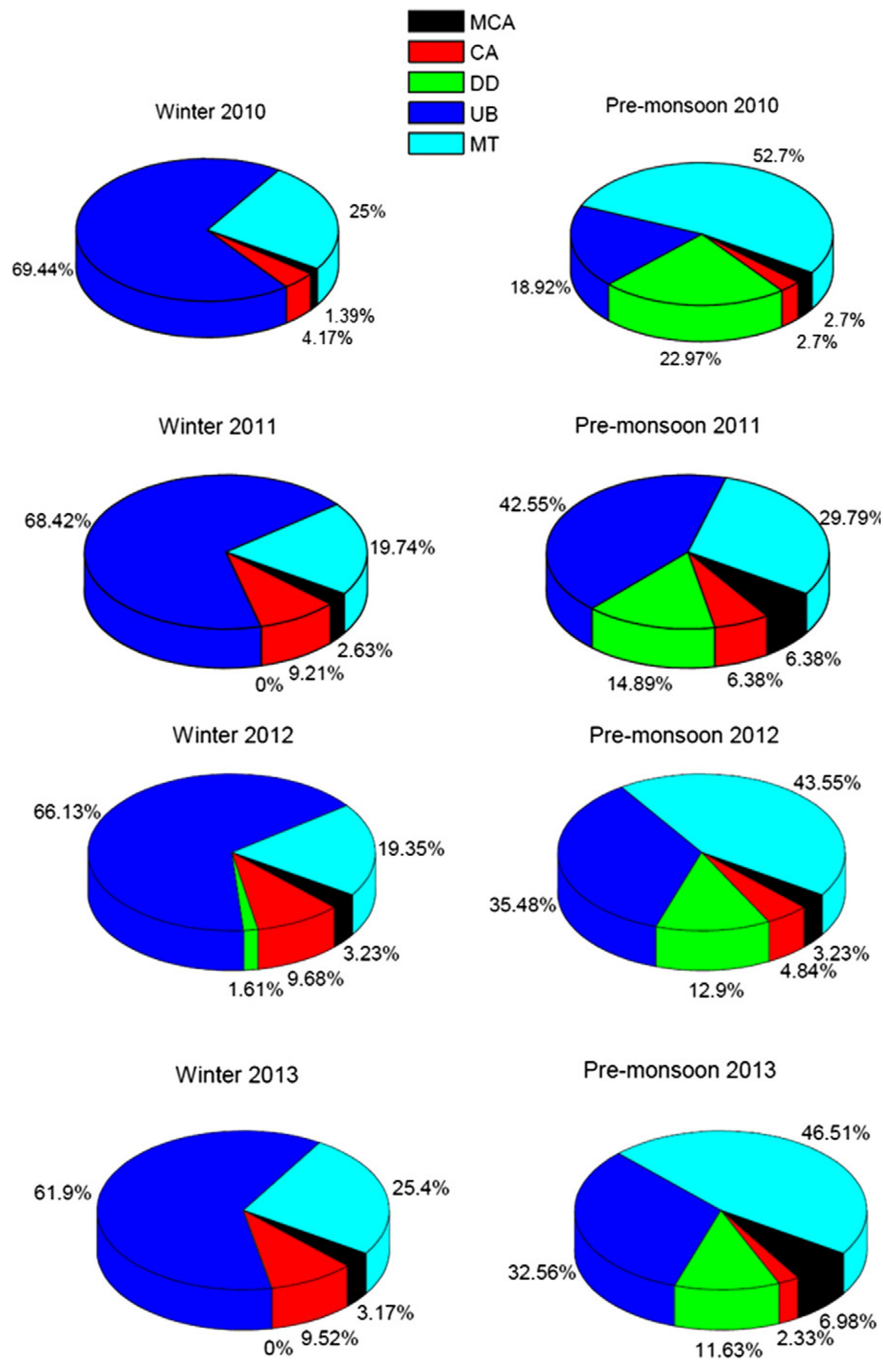

Fig. 7. Pie diagrams showing seasonal fraction of each aerosol type viz., continental average (CA), marine continental average (MCA), urban/industrial and biomass burning (UI/B), desert dust (DD) and mixed type (MT) over Pune during 2010–13.

Moorthy et al., (2008) have reported the influence of the anthropogenic pollution (accumulation-mode aerosols, mostly UI/B type) from the industrialized areas of the Indian west coast, which was found to have a spatial offshore extent of <100 km at the coast. As the wind speeds are generally low during the winter season, the transport of mineral dust (DD aerosols) is less significant. Also, the local trajectories are capable of contributing more to the UI/B type. On an average of 9–10% of background CA type is the result of aerosols generated locally under favorable meteorological conditions (clear sky and scanty rainfall). Under such meteorological conditions, it is probable that the particles may float for longer time in the atmosphere due to reduction in loss/removal processes and may undergo transformation in their size (Pathak et al., 2012).

During pre-monsoon seasons, MT is the dominant aerosol type followed by UI/B and DD, while the background aerosols are insignificant. The dominance of MT aerosols may be due to the dust emissions and transport in this season and the possible adhering of fine-mode pollution particles onto the surface of coarse-mode dust in the mixed aerosol. Since the majority of the aerosols belong to a mixed (or indeterminate) aerosol type, more attention must be paid to this type, as they arise as a result of independent processes. Thus, the mixing could be caused by primary small and large particles. On the other hand, the coarse-mode particles transported over Pune can easily be mixed with local pollution or with smoke biomass burning, increasing the AOD magnitude modulating its wavelength dependence. The air-masses (at all altitudes considered in the study) mainly from the arid regions in

North-Western India, Pakistan and Gulf countries are capable of carrying DD aerosols. However, the second highest dominance of UB may be due to biomass burning activities (mainly wheat crop and rice crop residue) in the pre-monsoon season which is mainly associated with shifting cultivation practices taking place in IGB region every year (Badarinath et al., 2004, 2008). Moreover, on the local level, in the vicinity of observing site, the biomass burning activity is also at its highest during pre-monsoon. The transportation from the Arabian Sea and the Indian Ocean results in significant percentage of MCA (6–8%) type during pre-monsoon as winds starts to blow from the NW/W and SW/S regions (Fig. 7).

The comparison of the present results with those reported over Hyderabad (Kaskaoutis et al., 2009), a typical urban location similar to that of Pune, reveals that the UI/B aerosol type is the highest contributor during winter and second highest contributor in pre-monsoon over both the places. The DD (high AOD desert dust over Hyderabad) aerosols are predominant in pre-monsoon and almost absent in winter over Pune. On the other hand, the other aerosol types exhibit different seasonal variations over the two locations. The difference in the observed seasonal contribution of aerosol types over Pune and Hyderabad may be attributed to the site location, meteorology, and topography, influences of air-masses and mixing of aerosols.

5. Summary and conclusions

The present study represents a quantitative characterization of AOD and AE within different air-mass types specific to Pune, India for the period 2010–2013. The salient features of the study are summarized below.

- The 2-D contour diagram of AERONET measured monthly mean $AOD_{500\ nm}$ over Pune exhibits a strong seasonal variation. This regular nature of annul/seasonal variations of AOD would be due to the influence of perturbing factors which are regular in nature, at least on a regional scale. The spatial climatology of MODIS (Terra) measured yearly mean $AOD_{550\ nm}$ over the Indian subcontinent for the period 2004–13 depicts that there is large gradient in AOD from South to North.
- Five potential advection pathways viz., NW/W, SW/S, N, SE/E and L have been identified over the observing site by employing the NOAA-HYSPLIT air mass back trajectory analysis.
- Dominance of UB type in the winter season for all the years (i.e. 2010–2013) may be attributed to both local and transported aerosols. On an average, about 9–10% of background CA type is the result of aerosols generated locally under favorable meteorological conditions. During pre-monsoon seasons, MT is the dominant aerosol type followed by UB and DD, while the background aerosols are insignificant. The transport from Arabian Sea and Indian Ocean results in significant percentage of MCA (6–8%) type during pre-monsoon as winds starts to blow from the NW/W and SW/S regions.
- In winter, sector SE/E, a representative of air masses traversed over Bay of Bengal and Eastern continental Indian region has relatively small AOD ($\tau_{p\lambda} = 0.43 \pm 0.13$) and high AE ($\alpha = 1.19 \pm 0.15$). These values imply the presence of accumulation/sub-micron size anthropogenic aerosols. During pre-monsoon, aerosols from the NW/W sector has a high average AOD ($\tau_{p\lambda} = 0.61 \pm 0.21$), and a low AE ($\alpha = 0.54 \pm 0.14$) indicating an increase in the loading of coarse-mode particles over Pune.
- Frequency analysis reveals that $AOD_{500\ nm}$ for NW/W air-masses lies between 0.3 and 0.7 in 92% of all cases, with a peak frequency at 0.5 and corresponding histogram of AE for arid air-mass peaks at 0.5 with a range of 0.1 to 1.4. SW/S air-masses tend to have low AODs (<0.5; 81% of occurrences) with corresponding AE having peak at 0.7. Also, SW/S air masses show a bimodal type of distribution with peak frequencies at AE values of 0.4 and 0.5. This clearly indicates the influence of mixed type aerosols consisting of coarse (Sea salt) and fine-mode (anthropogenic) aerosols. The SE/E sector histogram has a peak AE at 0.5 and 1.0. The N sector air-masses have AODs ranging from 0.3 to 0.6 and AE between 0.8 and 1.4. The local air-masses also have broad range of AOD variation i.e. 0.2–1.0 and corresponding AE having a peak at 1.2 and a range of 0.8–1.4.

Acknowledgments

Authors acknowledge the support and encouragement received from the Principal, Nowrosjee Wadia College, Pune (India) and the Honorable Vice Chancellor, and Pro-Vice Chancellor, Amity University, Gurgaon (Manesar), India. The work carried out has been funded by the Honorable Director, ISRO-UoP Space Technology, Savitribai Phule Pune University, under ISRO-RESPOND Program of the Indian Space Research Organization, Dept. of Space, and Government of India (Grant number: GOI-A-337(B) 95). We acknowledge NOAA Air Resources Laboratory for providing the HYSPLIT transport and dispersion model (http://www.arl.noaa.gov/). MODIS data were obtained from the Level 3 and Atmosphere Archive and Distribution System (LAADS) at Goddard Space Flight Center (GSFC), (http://ladsweb.nascom.nasa.gov/data/). Authors thank the AERONET federation, AERONET scientific team and Principal Investigator Dr. P.C.S. Devara for Pune AERONET data. Thanks are also due to the editor and anonymous reviewers for their critical comments and insightful suggestions which helped to improve the clarity and scientific content of the original article.

References

Aher, G.R., Sen, P.N., Agashe, V.V., 2000. Effect of boundary layer circulation on aerosol characteristics. In: Beig, G. (Ed.), Proc. Int'l Workshop on Long Term Changes & Trends in the Atmosphere. vol. I. New Age International Publisher, New Delhi, pp. 280–292.

Aher, G.R., Pawar, G.V., Gupta, P., Devara, P.C.S., 2014. Effect of major dust storm on optical, physical, and radiative properties of aerosols over coastal and urban environments in Western India. Int. J. Remote Sens. 35, 871–903. http://dx.doi.org/10.1080/01431161.2013.873153.

Alam, K., Blaschke, T., Madl, P., Mukhtar, A., Hussain, M., Trautmann, T., Rehman, S., 2011a. Aerosol size distribution and mass concentration measurements in various cities of Pakistan. J. Environ. Monitor. 13, 1944–1952.

Alam, K., Trautmann, T., Blaschke, T., 2011b. Aerosol optical properties and radiative forcing over mega-city Karachi. Atmos. Res. 101, 773–782.

Aloysius, M., Mohan, M., Babu, S.S., Nair, V.S., Parameswaran, K., Moorthy, K.K., 2008. Influence of circulation parameters on the AOD variations over Bay of Bengal during ICARB. J. Earth Syst. Sci. 117 (S1), 353–360.

Ångström, A., 1961. Techniques of determining the turbidity of the atmosphere. Tellus 13, 214–223.

Babu, S.S., Chaubey, J.P., Moorthy, K.K., Gogoi, M.M., Kompalli, S.K., et al., 2011. High-altitude (4520 m amsl) measurements of black carbon aerosols over western trans-Himalayas: seasonal heterogeneity and source apportionment. J. Geophys. Res. 116, D24201. http://dx.doi.org/10.1029/2011JD016722.

Babu, S.S., Manoj, M.R., Krishna Moorthy, K., Gogoi, M.M., Nair, V.S., Kompalli, S.K., Satheesh, S.K., Niranjan, K., Ramagopal, K., Bhuyan, P.K., Singh, D., 2013. Trends in aerosol optical depth over Indian region: potential causes and impact indicators. J. Geophys. Res. Atmos. 118, 1–13. http://dx.doi.org/10.1002/2013JD020507.

Badarinath, K.V.S., Latha, K.M., Kiran Chand, T.R., Gupta, P.K., Ghosh, A.B., Jain, S.L., Gera, B.S., Singh, R., Sarkar, A.K., Singh, N., Parmar, R.S., Koul, S., Kohli, R., Nath, S., Ojha, V.K., Singh, G., 2004. Characterization of aerosols from biomass burning: a case study from Mizoram (Northeast), India. Chemosphere 54, 167–175.

Badarinath, K.V.S., Kharol, S.K., Prasad, V.K., Sharma, A.R., Reddi, E.U.B., Kambezidis, H.D., Kaskaoutis, D.G., 2008. Influence of natural and anthropogenic activities on UV Index variations—a study over tropical urban region using ground based observations and satellite Data. J. Atmos. Chem. 59, 219–236.

Badarinath, K.V.S., Kharol, S.K., Kaskaoutis, D.G., Sharma, A.R., Ramaswamy, V., Kambezidis, H.D., 2010. Long range transport of dust aerosols over Arabian Sea and Indian region—a case study using satellite data and ground-based measurements. Glob. Planet. Chang. 72, 164–181.

Bahrmann, C.P., Saxena, V.K., 1998. Influence of air mass history on black carbon concentrations and regional climate forcing in southeastern United States. J. Geophys. Res. 103, 23153–23161.

Bond, T.C., Doherty, S.J., Fahey, D.W., Forster, P.M., Berntsen, T., DeAngelo, B.J., Flanner, M.G., Ghan, S., Käarcher, B., Koch, D., Kinne, S., Kondo, Y., Quinn, P.K., Sarofim, M.C., Schultz, M.G., Schulz, M., Venkataraman, C., Zhang, H., Zhang, S., Bellouin, N., Guttikunda, S.K., Hopke, P.K., Jacobson, M.Z., Kaiser, J.W., Klimont, Z., Lohmann, U., Schwarz, J.P., Shindell, D., Storelvmo, T., Warren, S.G., Zender, C.S., 2013. Bounding the role of black carbon in the climate system: a scientific assessment. J. Geophys. Res. Atmos. 118, 5380–5552. http://dx.doi.org/10.1002/jgrd.50171.

Cabello, M., Orza, J., A. G., Galiano, V., Ruiz, G., 2008. Influence of meteorological input data on back trajectory cluster analysis—a seven-year study for southeastern Spain. Adv. Sci. Res. 2, 65–70.

Cape, J.N., Methven, J., Hudson, L.E., 2000. The use of trajectory cluster analysis to interpret trace gas measurements at Mace Head, Ireland. Atmos. Environ. 34, 3651–3663.

Chakravarty, K., Mukhopadhyay, P., Taraphdar, S., 2011. Cloud microphysical properties as revealed by the CAIPEEX and satellite observations and evaluation of a cloud system resolving model simulation of contrasting large scale environments. J. Atmos. Sol. Terr. Phys. 73, 1790–1797.

Dani, K.K., Raj, P.E., Devara, P.C.S., Pandithurai, G., Sonbawane, S.M., Maheshkumar, R.S., Saha, S.K., Jaya Rao, Y., 2012. Long term trends and variability in measured multi-spectral aerosol optical depth over a tropical urban station in India. Int. J. Climatol. 32, 153–160. http://dx.doi.org/10.1002/joc.2250.

Das, S.K., Jayaraman, A., Misra, A., 2008. Fog-induced variations in aerosol optical and physical properties over the Indo-Gangetic Basin and impact to aerosol radiative forcing. Ann. Geophys. 26, 1345–1354. http://dx.doi.org/10.5194/angeo-26-1345-2008.

Devara, P.C.S., Raj, P.E., Sharma, S., Maheskumar, R.S., 1994. Lidar-observed long-term variations in urban aerosol characteristics and their connection with meteorological parameters. Int. J. Climatol. 14, 581–591.

Devara, P.C.S., Maheshkumar, R.S., Earnest Raj, P., Dani, K.K., Sonbawne, S.M., 2001. Some features of columnar aerosol optical depth, ozone and precipitable water content observed over land during the INDOEXIFP99. Meteorol. Z. 10, 901–908.

Dey, S., Tripathi, S.N., Singh, R.P., Holben, B.N., 2004. Influence of dust storms on aerosol optical properties over the Indo-Gangetic basin. J. Geophys. Res. 109, D20211. http://dx.doi.org/10.1029/2004JD004924.

Dı'az, A.M., Dı'az, J.P., Expo'sito, F.J., Herna' ndez-Leal, P.A., Savoie, D., Querol, X., 2006. Air masses and aerosols chemical components in the free troposphere at the subtropical northeast Atlantic region. J. Atmos. Chem. 53, 63–90.

diSarra, A., Di Iorio, T., Cacciani, M., Fiocco, G., Fu'a, D., 2001. Saharan dust profiles measured by lidar at Lampedusa. J. Geophys. Res. 106, 10335–10348.

Dorling, S.R., Davies, T.D., Pierce, C.E., 1992. Cluster analysis: a technique for estimating the synoptic meteorological controls on air and precipitation chemistry—method and applications. Atmos. Environ. 26, 2575–2581.

Draxler, R.R., Hess, G.D., 1988. An overview of the HYSPLIT 4 modelling system for trajectories, dispersion, and deposition. Aust. Meteorol. Mag. 47 (295-208).

Dubovik, O., Holben, B.N., Eck, T.F., Smirnov, A., Kaufman, Y.J., King, M.D., Tanre, D., Slutsker, I., 2002. Variability of absorption and optical properties of key aerosol types observed in worldwide locations. J. Atmos. Sci. 59, 590–608.

Dubovik, O., Lapyonok, T., Kaufman, Y.J., Chin, M., Ginoux, P., Kahn, R.A., Sinyuk, A., 2008. Retrieving global aerosol sources from satellites using inverse modeling. Atmos. Chem. Phys. 8, 209–250. http://dx.doi.org/10.5194/acp-8-209-2008.

Eck, T.F., Holben, B.N., Reid, J.S., Dubovik, O., Smirnov, A., O'Neill, N.T., Slutsker, I., Kinne, S., 1999. Wavelength dependence of the optical depth of biomass burning, urban, and desert dust aerosols. J. Geophys. Res. 104, 31333–31349.

El-Askary, H., Gautam, R., Kafatos, M., 2004. Monitoring of dust storms over Indo-Gangetic Basin. J. Indian Soc. Remote Sens. 32, 121–124.

El-Askary, H., Gautam, R., Singh, R., Kafatos, M., 2006. Dust storms detection over the Indo-Gangetic basin using multi sensor data. Adv. Space Res. 37, 728–733.

El-Metwally, M., Alfaro, S.C., Abdel, M.W., Chatenet, B., 2008. Aerosol characteristics over urban Cairo: seasonal variations as retrieved from Sun Photometer. J. Geophys. Res. 113, D14219. http://dx.doi.org/10.1029/2008JD009834.

Estelle's, V.J., Martı'nez-Lozano, A., Utrillas, M.P., 2007. Influence of air mass history on the columnar aerosol properties at Valencia, Spain. J. Geophys. Res. 112, D15211. http://dx.doi.org/10.1029/ 2007JD008593.

Fleming Zoë, L., Monks Paul, S., Manning Alistair, J., 2012. Review: untangling the influence of air-mass history in interpreting observed atmospheric composition. Atmos. Res. 104–105, 1–39.

Formenti, P., et al., 2001. Saharan dust in Brazil and Suriname during the Large-Scale Biosphere–Atmosphere Experiment in Amazonia (LBA) — Cooperative LBA Regional Experiment (CLAIRE) in March 1998. J. Geophys. Res. 106, 14919–14934.

Forster, P., Ramaswamy, V., Artaxo, P., Berntsen, T., Betts, R., Fahey, D.W., Haywood, J., Lean, J., Lowe, D.C., Myhre, G., Nganga, J., Prinn, R., Raga, G., Schulz, M., Van Dorland, R., 2007. Changes in atmospheric constituents and in radiative forcing. In: Solomon, S., Qin, D., Manning, M., Chen, Z., Marquis, M., Averyt, K.B., Tignor, M., Miller, H.L. (Eds.), Climate Change 2007: The Physical Science Basis. Contribution of Working Group I to the Fourth Assessment Report of the Intergovernmental Panel on Climate Change. Cambridge University Press, Cambridge, UK and New York, NY.

Fraile, R., Calvo, A.I., Castro, A., Ferna'ndez-Gonza' lez, D., Garcı'a-Ortega1, E., 2006. The behavior of the atmosphere in long-range transport. Aerobiologia 22, 35–45. http://dx.doi.org/10.1007/s10453-005-9014-7.

Franke, K., Ansmann, A., Mu¨ ller, D., Althausen, D., Venkataraman, C., Reddy, M.S., Scheele, R., 2003. Optical properties of the Indo-Asian haze layer over the tropical Indian Ocean. J. Geophys. Res. 108, D24059. http://dx.doi.org/10.1029/2002JD002473.

Gautam, R., Hsu, N.C., Kafatos, M., Tsay, S.C., 2007. Influences of winter haze on fog/low cloud over Indo-Gangetic plains. J. Geophys. Res. 112, D05207. http://dx.doi.org/10.1029/2005JD007036.

Gautam, R., Hsu, N.C., Lau, K.-M., Kafatos, M., 2009a. Enhanced pre-monsoon warming over the Himalayan–Gangetic region from 1979 to 2007. J. Geophys. Res. 36, L07704. http://dx.doi.org/10.1029/2009GL037641.

Gautam, R., Liu, Z., Singh, R.P., Hsu, N.C., 2009b. Two contrasting dust-dominant periods over India observed from MODIS and CALIPSO data. Geophys. Res. Lett. 36, L06813. http://dx.doi.org/10.1029/2008GL036967.

Gautam, R., Liu, Z., Singh, R., Hsu, N.C., 2009c. Two contrasting dust-dominant periods over India observed from MODIS and CALIPSO data. Geophys. Res. Lett. 36, L06813. http://dx.doi.org/10.1029/2008GL036967.

Gerasopoulos, E., Andreae, M.O., Zerefos, C.S., Andreae, T.W., Balis, D., Formenti, P., Merlet, P., Amiridis, V., Papastefanou, C., 2003. Climatological aspects of aerosol optical properties in Northern Greece. Atmos. Chem. Phys. 3, 2025–2041. http://dx.doi.org/10.5194/acp-3-2025-2003.

Gogoi, M.M., Bhuyan, P.K., Moorthy, K.K., 2008. Estimation of the effect of long-range transport on seasonal variation of aerosols over northeastern India. Ann. Geophys. 26, 1365–1377.

Gorchakov, G.I., Sitnov, S.A., Sviridenkov, M.A., Semoutnikova, E.G., Emilenko, A.S., Isakov, A.A., Kopeikin, V.M., Karpov, A.V., Gorchakova, I.A., Verichev, K.S., Kurbatov, G.A., Ponomareva, T.Ya., 2014. Satellite and ground-based monitoring of smoke in the atmosphere during the summer wildfires in European Russia in 2010 and Siberia in 2012. Int. J. Remote Sens. 35, 5698–5721. http://dx.doi.org/10.1080/01431161.2014.945008.

Heintzenberg, J., et al., 2003. Arctic haze over central Europe. Tellus 55B, 796–807.

Hess, M., Koepke, P., Schult, I., 1998. Optical properties of aerosols and clouds: the software package OPAC. Bull. Am. Meteorol. Soc. 79, 831–844.

Holben, B., Eck, T., Slutsker, I., Tanre, D., Buis, J.P., et al., 1998. AERONET — a federated instrument network and data archive for aerosol characterization. Remote Sens. Environ. 66, 1–16.

Holben, B.N., Tanre, D., Smirnov, A., Eck, T.F., Slutsker, I., et al., 2001. An emerging ground-based aerosol climatology: aerosol optical depth from AERONET. J. Geophys. Res. 106, 12067–12097.

Jayaraman, A., Gadhavi, H., Ganguly, D., Misra, A., Ramachandran, S., Rajesh, T., 2006. Spatial variation in aerosol characteristics over central India observed during the February 2004 road campaign experiment. Atmos. Environ. 40, 6504–6515.

Jorba, O., Pérez, C., Rocadenbosch, F., Baldasano, J., 2004. Cluster analysis of 4-day back trajectories arriving in the Barcelona area (Spain) from 1997 to 2002. J. Appl. Meteorol. 43, 887–901.

Kabashnikov, V., Milinevsky, G., Chaikovsky, N., Miatselskaya, A., Danylevsky, V., Aculinin, A., Kalinskaya, D., Korchemkina, E., Bovchaliuk, A., Pietruczuk, A., Sobolewsky, P., Bovchaliuk, V., 2014. Localization of aerosol sources in East-European region by back-trajectory statistics. Int. J. Remote Sens. 35, 6993–7006. http://dx.doi.org/10.1080/01431161.2014.960621.

Kalapureddy, M.C.R., Kaskaoutis, D.G., Ernest Raj, P., Devara, P.C.S., Kambezidis, H.D., Kosmopoulos, P.G., Nastos, P.T., 2009. Identification of aerosol type over the Arabian Sea in the pre-monsoon season during the Integrated Campaign for Aerosols, Gases and Radiation Budget (ICARB). J. Geophys. Res. 114, D17203. http://dx.doi.org/10.1029/2009JD011826.

Kanakidou, M., Mihalopoulos, N., Kindap, T., Im, U., Vrekoussis, M., Gerasopoulos, E., Dermitzaki, E., Unal, A., Kocak, M., Markakis, K., Melas, D., Kouvarakis, G., Youssef, A.F., Richter, A., Hatzianastassiou, N., Hilboll, A., Ebojie, F., Wittrock, F., von Savigny, C., Burrows, J.P., Ladstaetter-Weissenmayer, A., Moubasher, H., 2011. Megacities as hotspots of air pollution in the East Mediterranean. Atmos. Environ. 45, 1223–1235.

Kanike, R.K., Sivakumar, V., Reddy, R.R., Gopal, R.R., Adesina, A.J., 2014. Identification and classification of different aerosol types over a subtropical rural site in Mpumalanga, South Africa: seasonal variation as retrieved from the AERONET Sun Photometer. Aerosol Air Qual. Res. 14, 108–123. http://dx.doi.org/10.4209/aaqr.2013.03.0079.

Kaskaoutis, D.G., Kambezidis, H.D., 2008. Comparison of the Angstrom parameters retrieval in different spectral ranges with the use of different techniques. Meteorol. Atmos. Phys. 99, 233–246.

Kaskaoutis, D.G., Kosmopoulos, P., Kambezidis, H.D., Nastos, P.T., 2007a. Aerosol climatology and discrimination of different types over Athens, Greece, based on MODIS data. Atmos. Environ. 41, 7315–7329.

Kaskaoutis, D.G., Kambezidis, H.D., Hatzianastassiou, N., Kosmopoulos, P.G., Badarinath, K.V.S., 2007b. Aerosol climatology: on the discrimination of aerosol types over four AERONET sites. Atmos. Chem. Phys. Discuss. 7, 6357–6411.

Kaskaoutis, D.G., Kambezidis, H.D., Hatzianastassiou, N., Kosmopoulos, P.G., Badarinath, K.V.S., 2007c. Aerosol climatology: dependence of the angstrom exponent on wavelength over four AERONET sites. Atmos. Chem. Phys. Discuss. 7, 7347–7397.

Kaskaoutis, D.G., Badarinath, K.V.S., Kharol, S.K., Sharma, A.R., Kambezidis, H.D., 2009. Variations in the aerosol optical properties and types over the tropical urban site of Hyderabad, India. J. Geophys. Res. 114, D22204. http://dx.doi.org/10.1029/2009JD012423.

Kaskaoutis, D.G., Kalapureddy, M.C.R., Moorthy, K.K., Devara, P.C.S., Nastos, P.T., Kosmopoulos, P.G., Kambezidis, H.D., 2010. Heterogeneity in pre-monsoon aerosol types over the Arabian Sea deduced from ship-borne measurements of spectral AODs. Atmos. Chem. Phys. 10, 4893–4908.

Kaskaoutis, D.G., Kharol Kumar, S., Sinha, P.R., Singh, R.P., Kambezidis, H.D., Sharma Rani, A., Badarinath, K.V.S., 2011. Extremely large anthropogenic-aerosol contribution to total aerosol load over the Bay of Bengal during winter season. Atmos. Chem. Phys. 11, 7097–7117. http://dx.doi.org/10.5194/acp-11-7097-2011.

Kaskaoutis, D.G., Kumar, S., Singh, R.P., Kharol, S.K., Sharma, S., Singh, M., Singh, A.K., Singh, A., Singh, D., 2014. Effects of crop residue burning on aerosol properties, plume characteristics, and long-range transport over northern India. J. Geophys. Res. 119, 5424–5444. http://dx.doi.org/10.1002/2013jd021357.

Kharol, S.K., Badarinath, K.V.S., Sharma, A.R., Kaskaoutis, D.G., Kambezidis, H.D., 2011. Multiyear analysis of Terra/Aqua MODIS aerosol optical depth and ground observations over tropical urban region of Hyderabad, India. Atmos. Environ. 45, 1532–1542.

Khemani, L.T., 1989. Physical and chemical characteristics of atmospheric aerosols in air pollution control. Encyclopedia of Environmental Control Technology. Vol. 2. Gulf Publ. Co., USA, pp. 401–452.

Khemani, L.T., Momin, G.A., Naik, M.S., Vijayakumar, R., Ramana Murty Bh, V., 1982. Chemical composition and size distribution of atmospheric aerosols over the Deccan Plateau, India. Tellus 34, 151–155.

Kim, D.H., Ramanathan, V., 2008. Solar radiation budget and radiative forcing due to aerosols and clouds. J. Geophys. Res. 113, D02203. http://dx.doi.org/10.1029/2007jd008434.

Kosmopoulos, P.G., Kaskaoutis, D.G., Nastos, P.T., Kambezidis, H.D., 2008. Seasonal variation of columnar aerosol optical properties over Athens, Greece, based on MODIS data. Remote Sens. Environ. 112, 2354–2366.
Krishnamurti, T.N., Jha, B., Prospero, J.M., Jayaraman, A., Ramanathan, V., 1998. Aerosol and pollutant transport over the tropical Indian Ocean during the January–February, 1996 pre-INDOEX cruise. Tellus Ser. B 50, 521–542.
Kulkarni, J.R., et al., 2012. Cloud aerosol interaction and precipitation enhancement experiment (CAIPEEX): overview and preliminary results. Curr. Sci. 102, 413–425.
Kumar, S., Kumar, S., Singh, A.K., Singh, R.P., 2012. Seasonal variability of atmospheric aerosol over the North Indian region during 2005–2009. Adv. Space Res. 50, 1220–1230.
Lelieveld, J., Berresheim, H., Borrmann, S., et al., 2002. Global air pollution crossroads over the Mediterranean. Science 298, 794–799.
Levy, R.C., Remer, L.A., Kleidman, R.G., Mattoo, S., Ichoku, C., Kahn, R., Eck, T.F., 2010. Global evaluation of the collection 5 MODIS dark-target aerosol products over land. Atmos. Chem. Phys. 10, 10399–10420.
Lin, I.I., Chen, J.P., Wong, G.T.F., Huang, C.W., Lien, C.C., 2007. Aerosol input to the South China Sea: results from the moderate resolution imaging spectroradiometer, the quick scatterometer, and the measurements of pollution in the troposphere sensor. Deep Sea Res., Part II 54, 1589–1601. http://dx.doi.org/10.1016/j.dsr2.2007.05.013.
Mayol-Bracero, O., Gabriel, R., Andreae, M., Kirchstetter, T., Novakov, T., Ogren, J., Sheridan, P., Streets, D., 2002. Carbonaceous aerosols over the Indian Ocean during INDOEX: chemical characterization, optical properties and probable sources. J. Geophys. Res. 107 (D19), 8030. http://dx.doi.org/10.1029/2000JD000039.
Methven, J., Evans, M., Simmonds, P., Spain, G., 2001. Estimating relationships between air mass origin and chemical composition. J. Geophys. Res. 106, 5005–5019.
Moorthy, K.K., Nair, P.R., Krishna Murthy, B.V., 1991. Size distribution of coastal aerosols; effects of local sources and sinks. J. Appl. Meteorol. 30, 844–852.
Moorthy, K.K., et al., 1999. Aerosol Climatology Over India. 1 — ISRO GBP MWR Network and Database, ISRO/GBP, SR-03-99.
Moorthy, K.K., Saha, A., Prasad, B.S.N., Niranjan, K., Jhurry, D., Pillai, P.S., 2001. Aerosol optical depths over peninsular India and adjoining oceans during the INDOEX campaigns: spatial, temporal, and spectral characteristics. J. Geophys. Res. 106, 28539–28554.
Moorthy, K.K., Babu, S.S., Satheesh, S.K., 2003. Aerosol spectral optical depths over the Bay of Bengal: role of transport. Geophys. Res. Lett. 30, 1249. http://dx.doi.org/10.1029/2002GL016520.
Moorthy, K.K., Sunilkumar, S.V., Pillai, P.S., Parameswaran, K., Nair, P.R., et al., 2005. Wintertime spatial characteristics of boundary layer aerosols over peninsular India. J. Geophys. Res. 110, D08207. http://dx.doi.org/10.1029/2004JD005520.
Moorthy, K.K., Nair, V.S., Babu, S.S., Satheesh, S.K., 2009. Spatial and vertical heterogeneities in aerosol properties over oceanic regions around India: implications for radiative forcing. Q. J. R. Meteorol. Soc. 135, 2131–2145.
Moorthy, K.K., Satheesh, S.K., Babu, S.S., Dutt, C.B.S., 2008. Integrated Campaign for Aerosols, gases and Radiation Budget (ICARB): An overview. J. Earth Syst. Sci. 117, 243–262.
Moorthy, Krishna K., Babu, S.S., Manoj, M.R., Satheesh, S.K., 2013. Buildup of aerosols over the Indian Region. Geophys. Res. Lett. 40, 1011–1014. http://dx.doi.org/10.1002/grl.50165.
Ogunjobi, K.O., He, Z., Simmer, C., 2008. Spectral aerosol optical properties from AERONET Sun photometric measurements over West Africa. Atmos. Res. 88, 89–107.
Pace, G., di Sarra, A., Meloni, D., Piacentino, S., Chamard, P., 2006. Aerosol optical properties at Lampedusa (Central Mediterranean), 1. Influence of transport and identification of different aerosol types. Atmos. Chem. Phys. 6, 697–713.
Padmakumari, B., Maheshkumar, R.S., Harikrishan, G., Morwal, S.B., Prabha, T.V., Kulakarni, J.R., 2013. In situ measurements of aerosol vertical and spatial distributions over continental India during the major drought year 2009. Atmos. Environ. 80, 107–121. http://dx.doi.org/10.1016/j.atmosenv.2013.07.064.
Pandithurai, G., Pinker, R.T., Devara, P.C.S., Takamura, T., Dani, K.K., 2007. Seasonal asymmetry in diurnal variation of aerosol optical characteristics over Pune Western India. J. Geophys. Res. 112, D08208. http://dx.doi.org/10.1029/2006JD007803.
Pathak, B., Bhuyan, P.K., Gogoi, M., Bhuyan, K., 2012. Seasonal heterogeneity in aerosol types over Dibrugarh-North-Eastern India. Atmos. Environ. 47, 307–315.
Pawar, G.V., Devara, P.C.S., More, S.D., Pradeep Kumar, P., Aher, G.R., 2012. Determination of aerosol characteristics and direct radiative forcing at Pune. Aerosol Air Qual. Res. 12, 1166–1180. http://dx.doi.org/10.4209/aaqr.2011.09.0157.
Penner, J.E., Andreae, M., Annegarn, H., Barrie, L., Feichter, J., Hegg, D., Jayaraman, A., Leaitch, R., Murphy, D., Nganga, J., Pitari, G., 2001. Climate Change 2001: The Scientific Assessment. Cambridge University Press, New York, NY, pp. 289–348.
Penner, J.E., Xu, L., Wang, M., 2011. Satellite methods underestimate indirect climate forcing by aerosols. Proc. Natl. Acad. Sci. 108, 13404–13408. http://dx.doi.org/10.1073/pnas.1018526108.
Pérez, C., Sicard, M., Jorba, O., Comerón, A., Baldasano, J.M., 2004. Summertime recirculations of air pollutants over the north-eastern Iberian coast observed from systematic EARLINET lidar measurements in Barcelona. Atmos. Environ. 38, 3983–4000.
Pillai, P.S., Moorthy, K.K., 2001. Aerosol mass-size distributions at a tropical coastal environment: response to mesoscale and synoptic processes. Atmos. Environ. 35, 4099–4112.
Prasad, A.K., Singh, R.P., Singh, A., 2004. Variability of aerosol optical depth over Indian subcontinent using MODIS data. J. Indian Soc. Remote Sens. 32, 313–316.
Querol, X., Alastuey, A., de la Rosa, J., Sa'nchez de la Campa, A., Plana, F., Ruiz, C.R., 2002. Source apportionment analysis of atmospheric particulates in an industrialized urban site in southwestern Spain. Atmos. Environ. 36, 3113–3125.
Quinn, P.K., Coffman, D.J., Bates, T.S., Miller, T.L., Johnson, J.E., Welton, E.J., Neusu¨ss, C., Miller, M., Sheridan, P.J., 2002. Aerosol optical properties during INDOEX 1999: means, variability, and controlling factors. J. Geophys. Res. 107 (D19), 8020. http://dx.doi.org/10.1029/2000JD000037.
Ramanathan, V., Crutzen, P.J., Lelieveld, J., Mitra, A.P., et al., 2001. Indian Ocean experiment: an integrated analysis of the climate forcing and the effects of the great Indo-Asian haze. J. Geophys. Res. 106, 28371–28398.
Reiner, T., Sprung, D., Jost, C., Gabriel, R., Mayol-Bracero, O., Andreae, M., Campos, T., Shetter, R., 2001. Chemical characterization of pollution layers over the tropical Indian Ocean: signatures of biomass burning emissions. J. Geophys. Res. 106 (D22), 28497–28510.
Rodriguez, S., Querol, X., Alastues, A., Kallos, G., Kakaliagou, O., 2001. Saharan dust contribution to PM10 and TSP levels in southern and eastern Spain. Atmos. Environ. 35, 2433–2447.
Sa'nchez, M.L., Pascual, D., Ramos, C., Pe' rez, I., 1990. Forecasting particulate pollutant concentrations in a city from meteorological variables and regional weather patterns. Atmos. Environ. 24A, 1509–1519.
Safai, P.D., Rao, P.S.P., Momin, G.A., Ali, K., Chate, D.M., Praveen, P.S., Devara, P.C.S., 2005. Variation in the chemistry of aerosols in two different winter seasons at Pune and Sinhagad, India. Aerosol Air Qual. Res. 5, 115–126.
Santese, M., De Tomasi, F., Perrone, M.R., 2008. Advection patterns and aerosol optical and microphysical properties by AERONET over south-east Italy in the central Mediterranean. Atmos. Chem. Phys. 8, 1881–1896.
Sharma, M., Kaskaoutis, D.G., Singh, R.P., Singh, S., 2014. Seasonal variability of atmospheric aerosol parameters over Greater Noida using ground sun photometer observations. Aerosol Air Qual. Res. 14, 608–622. http://dx.doi.org/10.4209/aaqr.2013.06.0219.
Singh, S., Nath, S., Kohli, R., Singh, R., 2005. Aerosols over Delhi during premonsoon months: characteristics and effects on surface radiation forcing. Geophys. Res. Lett. 32, L13808. http://dx.doi.org/10.1029/2005GL023062.
Sinha, P.R., Manchanda, R.K., Subbaro, J.V., Dumka, U.C., Sreenivasan, S., Babu, S.S., Moorthy, K.K., 2011. Spatial distribution and vertical structure of the MABL aerosols over the Bay of Bengal during winter: results from W-ICARB experiment. J. Atmos. Sol. Terr. Phys. 73, 430–438.
Sinha, P.R., Kaskaoutis, D.G., Manchanda, R.K., Sreenivasan, S., 2012. Characteristics of aerosols over Hyderabad in southern Peninsular India: synergy in the classification techniques. Ann. Geophys. 30, 1393–1410.
Smirnov, A., Royer, A., O'Neill, N.T., Tarussov, A., 1994. A study of the link between synoptic airmass type and atmospheric optical parameters. J. Geophys. Res. 99, 20967–20982.
Smirnov, A., Villevalde, Yu, O'Neill, N.T., Royer, A., Tarussov, A., 1995. Aerosol optical depth over the oceans: analysis in terms of synoptic air mass types. J. Geophys. Res. 100, 16639–16650.
Smirnov, A., Holben, B.N., Eck, T.F., Dubovik, O., Slutsker, I., 2000. Cloud-screening and quality control algorithms for the AERONET database. Remote Sens. Environ. 73, 337–349. http://dx.doi.org/10.1016/S0034-4257(00)00109-7.
Smirnov, A., Holben, B.N., Kaufman, Y.J., Dubovik, O., Eck, T.F., Slutsker, I., Pietras, C., Halthore, R., 2002. Optical properties of atmospheric aerosol in maritime environments. J. Atmos. Sci. 59, 501–523.
Stohl, A., Eckhardt, S., Forster, C., James, P., Spichtinger, N., Seibert, P., 2002a. A replacement for simple back trajectory calculations in the interpretation of atmospheric trace substance measurements. Atmos. Environ. 36, 4635–4648.
Stohl, A., Eckhardt, S., Forster, C., James, P., Spichtinger, N., 2002b. On the pathways and timescales of intercontinental air pollution transport. J. Geophys. Res. 107 (D23), 4684. http://dx.doi.org/10.1029/2001JD001396.
Toledano, C., 2005. Aerosol Climatology Through the Characterization of Optical Properties and Air Masses at the "El Arenosillo" Station of the AERONET Network. (Ph.D. thesis). University of Valladolid, Valladolid, Spain, p. 239.
Toledano, C., Cachorro, V.E., Berjon, A., Sorribas, M., Vergaz, R., de Frutos, A., Anton, M., Gausa, M., 2006. Aerosol optical depth at ALOMAR observatory (Andoya, Norway) in summer 2002 and 2003. Tellus 58B, 218–228.
Tyson, P.D., Garstang, M., Swap, R., Kallberg, P., Edwards, N., 1996. An air transport climatology for subtropical southern Africa. Int. J. Climatol. 16, 256–291.
Vergaz, R., Cachorro, V.E., de Frutos, A.M., 2002. Comparison between classifications of aerosol types in the Gulf of Cadiz area, based on their spectral behavior and on the calculation of back trajectories. Proc. Third Spanish–Portuguese Assembly on Geodesy and Geophysics. vol. II. Instituto. Nacional de Meteorologı'a, Valencia, Spain, p. 1229.
Vergaz, R., Cachorro, V.E., Vilaplana, J.M., de la Morena, B.A., 2005. Columnar characteristics of aerosols in the maritime area of the Cadiz Gulf (Spain). Int. J. Climatol. 25, 1781–1804.
Vijayakumar, K., Devara, P.C.S., Simha, C.P., 2012. Aerosol features during drought and normal monsoon years: a study undertaken with multi-platform measurements over a tropical urban site. Aerosol Air Qual. Res. 12, 1444–1458.
Vijayakumar, K., Devara, P.C.S., Sonbawne, S.M., 2014. Type-segregated aerosol effects on regional monsoon activity: a study using ground-based experiments and model simulations. Atmos. Environ. 99, 650–659.
Xu, J., Geng, F., Gao, W., Zhen, C., 2009. Aerosol scattering coefficient and the factors affecting them in Shanghai Pudong. Acta Sci. Circumst. 30, 211–216.